Lichstein Jeremy (Orcid ID: 0000-0001-5553-6142)
Zhang Tao (Orcid ID: 0000-0001-7135-1762)
Farrior Caroline (Orcid ID: 0000-0001-8999-4264)

Effects of water limitation and competition on tree carbon allocation in an Earth system modeling framework

Jeremy W. Lichstein[1*], Tao Zhang[1], Ensheng Weng[2], Caroline E. Farrior[3], Ray Dybzinski[4], Sergey Malyshev[5], Elena Shevliakova[5], Richard A. Birdsey[6], Stephen W. Pacala[7]

[1]Department of Biology, University of Florida, Gainesville, FL 32611, USA
[2]Center for Climate Systems Research, Columbia University, and NASA Goddard Institute for Space Studies, New York, NY 10025, USA
[3]Department of Integrative Biology, University of Texas at Austin, Austin, TX 78712, USA
[4]School of Environmental Sustainability, Loyola University Chicago, Chicago, IL 60660, USA
[5]Cooperative Institute for Climate Science, Princeton University, and NOAA Geophysical Fluid Dynamics Laboratory, Princeton, NJ 08544, USA
[6]Woodwell Climate Research Center, Falmouth, MA 02540, USA
[7]Department of Ecology & Evolutionary Biology, Princeton University, Princeton, NJ 08544, USA

*Corresponding author: Jeremy W. Lichstein (jlichstein@ufl.edu)

ORCID IDs

Jeremy W. Lichstein:	0000-0001-5553-6142
Tao Zhang:	0000-0001-7135-1762
Ensheng Weng:	0000-0002-1858-4847
Caroline E. Farrior:	0000-0001-8999-4264
Ray Dybzinski:	0000-0002-1712-1875
Sergey Malyshev:	0000-0001-6259-1043
Elena Shevliakova:	0000-0003-4910-2166
Richard A. Birdsey:	0000-0002-3595-1100
Stephen Pacala:	0000-0003-4450-6532

Effects of water limitation and competition on tree carbon allocation in an Earth system modeling framework

Jeremy W. Lichstein[1*], Tao Zhang[1], Ensheng Weng[2], Caroline E. Farrior[3], Ray Dybzinski[4], Sergey Malyshev[5], Elena Shevliakova[5], Richard A. Birdsey[6], Stephen W. Pacala[7]

[1]Department of Biology, University of Florida, Gainesville, FL 32611, USA

This is the author manuscript accepted for publication and has undergone full peer review but has not been through the copyediting, typesetting, pagination and proofreading process, which may lead to differences between this version and the Version of Record. Please cite this article as doi: 10.1111/1365-2745.14416

[2]Center for Climate Systems Research, Columbia University, and NASA Goddard Institute for Space Studies, New York, NY 10025, USA

[3]Department of Integrative Biology, University of Texas at Austin, Austin, TX 78712, USA

[4]School of Environmental Sustainability, Loyola University Chicago, Chicago, IL 60660, USA

[5]Cooperative Institute for Climate Science, Princeton University, and NOAA Geophysical Fluid Dynamics Laboratory, Princeton, NJ 08544, USA

[6]Woodwell Climate Research Center, Falmouth, MA 02540, USA

[7]Department of Ecology & Evolutionary Biology, Princeton University, Princeton, NJ 08544, USA

*Corresponding author: Jeremy W. Lichstein (jlichstein@ufl.edu)

Article type: Research article

ABSTRACT

1) Earth system models (ESMs) have a limited capacity to represent plant functional diversity and shifts in trait distributions. Approaches to improving the representation of this complexity in ESMs include (*i*) optimality-based approaches that predict trait-environment responses and (*ii*) explicitly modeling coexistence and community assembly. These approaches are expected to converge only when optimality-based approaches identify competitively dominant strategies, which often differ from strategies that maximize ecosystem functioning or fitness components in monoculture.
2) We used two models, LM3-PPA (a vegetation demographic model designed as an ESM component) and BiomeE (a computationally efficient analog for LM3-PPA), to explore how water limitation affects carbon allocation strategies of canopy trees. We compared competitive allocation strategies and those that maximize biomass or productivity in monoculture. We did not explicitly model coexistence or community assembly. Rather, we used model experiments to identify competitive and maximizing strategies in a two-dimensional trait space under different precipitation and mortality scenarios.
3) At 10 eastern USA locations, we simulated historical, wet, and dry climate scenarios, novel drought, and three different mortality scenarios (low, medium, or high sensitivity to water deficit). For each site and scenario, we identified the competitive strategy and three maximizing strategies (maximum biomass, productivity, or drought-tolerance).
4) Root:leaf ratios tended to increase and leaf area tended to decrease with increasing water stress (increasing water limitation and its effects on mortality). However, relative to maximizing strategies, competitive strategies shifted towards greater allocation to roots and leaves with increasing water stress.

5) Competitive overinvestments (greater allocation to roots and leaves by competitive strategies compared to maximizing strategies) were robust across different modeling contexts, including vegetation parameter sets (*Acer* vs. *Populus*), models (LM3-PPA vs. BiomeE), and uncalibrated vs. calibrated BiomeE versions.
6) Synthesis: The theoretical prediction that competitive and maximizing allocation strategies differ under water limitation is confirmed for a demographic model designed as an ESM component. Optimality-based trait predictions can simplify representing trait diversity in ESMs but do not always correspond to competitive outcomes. Explicitly modeling coexistence and community assembly in ESMs is challenging but is likely the most general approach to representing trait diversity.

KEY WORDS

drought, dynamic global vegetation model, evolutionarily stable strategy, perfect plasticity approximation, plant water deficit, trait-based model, vegetation demographic model

INTRODUCTION

The global land carbon (C) sink sequestered ~30% of anthropogenic C emissions over recent decades (Friedlingstein et al. 2023), with much of this sink likely residing in forests (Pan et al. 2011a). However, there is large uncertainty in how forest C storage will respond to future climate change and drought (Friedlingstein et al. 2006, Sitch et al. 2008, Reichstein et al. 2013, Anderegg et al. 2015, Hubau et al. 2020). Thus, there is an urgent need to better understand forest responses to water limitation and to incorporate this understanding into terrestrial ecosystem models, including dynamic global vegetation models (DGVMs) (Sitch et al. 2008) and the land components of Earth system models (ESMs) (Arora et al. 2020), some of which are also DGVMs.

Two limitations of most DGVMs and ESMs are (*i*) the simplistic representation of plant functional diversity, with ~10 discrete plant functional types (PFTs) typically used to represent global biodiversity, and (*ii*) the absence or limited representation of processes related to plant demography and competition (Moorcroft 2006). There is growing interest in addressing these limitations through enhanced representations of trait diversity (e.g., Scheiter et al. 2013, Wullschleger et al. 2014, Fisher et al. 2015, Sakschewski et al. 2015, Langan et al. 2017, Dantas de Paula et al. 2021) and individual- or cohort-based representations of resource competition and demography (e.g., Friend et al. 1997, Moorcroft et al. 2001, Smith et al. 2001, Weng et al. 2015, Koven et al. 2020). Overcoming these limitations allows the simulated distribution of traits across space and time to emerge from bottom-up mechanisms, rather than being prescribed from empirical correlations or bioclimatic envelopes that may not apply under future novel conditions (Fisher et al. 2015).

Despite the growing interest in enhanced representations of trait variation, competition, and demography, these features are not included in most ESMs. For example, of the 11 ESMs in the most recent coupled model intercomparison project (Arora et al. 2020), only three include dynamic vegetation (i.e., non-static PFT biogeography), and only one (GFDL-ESM4) includes demographic processes. The simplistic representation of ecosystem dynamics in most ESMs is problematic, given the potential for demography and size-structured resource competition to substantially affect model outcomes (Moorcroft et al. 2001, Weng et al. 2015, 2019, Levine et al. 2016, Sakschewski et al. 2016, Koven et al. 2020).

One challenge associated with simulating demography-based trait distributions is maintaining the functional diversity upon which competition can act (Fisher and Koven 2020, Franklin et al. 2020). Forest dynamics models that capture the environmental heterogeneity created by canopy disturbances allow multiple successional types to coexist (e.g., Pacala et al. 1996, Moorcroft et al. 2001, Gravel et al. 2010, Falster et al. 2017, Detto et al. 2022), but maintaining additional axes of diversity (e.g., related to hydraulic niches) requires either 'seeding in' propagules from pre-determined trait distributions (Sakschewski et al. 2016) or incorporating additional mechanisms into already-complex ecosystem models (Scheiter et al. 2013, Fisher and Koven 2020).

An alternative to explicitly representing diversity and competition is to use optimality-based approaches to dynamically update the traits in each location (e.g., model grid cell) so as to maximize or track fitness functions (Franklin et al. 2020). This approach requires assumptions about the relevant time-scale of response but is otherwise relatively straightforward if empirically-supported analytical formulations are available (Harrison et al. 2021) or if maximizing a fitness proxy (e.g., growth) in the absence of interspecific competition (i.e., in

monoculture; Caldararu et al. 2020) correctly identifies the competitively optimal traits (the evolutionary stable strategy, or ESS; Franklin et al. 2012). However, competitive optimization often requires special attention. In particular, competition for belowground resources often leads plants to overinvest in fine roots, such that the most competitive C allocation strategy differs from 'maximizing strategies' that optimize ecosystem functioning or fitness components in monoculture (King 1993, Gersani et al. 2001, Craine 2006). Analytical solutions to competitive optimization of plant C allocation have been derived in some tractable models (e.g., Dybzinski et al. 2011, Farrior et al. 2013, 2015), but it is not clear if or how these results can be translated to more complex and realistic models such as ESMs, which are analytically intractable and computationally demanding.

Accurately representing the outcome of competition and demography in ESMs would require either (*i*) explicitly modeling the relevant processes; e.g., maintaining greater levels of trait diversity than has been accomplished to date in ESMs; or (*ii*) implicitly modeling the relevant processes; e.g., developing more general approaches to competitive optimization in complex models to accommodate cases where competitive and monoculture optimizations diverge (Franklin et al. 2012). Given the considerable challenges associated with implementing these advances in ESMs, it is important to better understand what would be gained from the investment. A starting point is to determine if, in an ESM context, competitive traits differ from optimal monoculture traits, as predicted by simpler models.

In this study, we use two demography-based DGVMs – LM3-PPA (Weng et al. 2015), which was designed as an ESM component, and BiomeE (Weng et al. 2019), a computationally efficient analog for LM3-PPA – to study C allocation strategies of canopy trees in response to water limitation. We use multi-strategy experiments to identify competitive traits and

monoculture experiments to identify maximizing traits. We do not explicitly model coexistence and community assembly. Rather, our study aims to understand some potential consequences of overcoming these challenges in ESMs. Previous work with LM3-PPA and BiomeE showed that competitive and maximizing strategies diverged in response to elevated CO_2 (Weng et al. 2015) and nitrogen limitation (Weng et al. 2019) and that predictions from simpler models (Farrior et al. 2013, Dybzinski et al. 2015) provided qualitative insights into the DGVM behaviors. Here, we extend this work to the context of water limitation.

In addition to C allocation, plant hydraulic traits (e.g., xylem anatomy and cavitation resistance) also play an important role in determining ecosystem responses to water limitation (McDowell et al. 2013, Christoffersen et al. 2016), but studying hydraulic trait variation is beyond the scope of our study. Nevertheless, our focus on tree C allocation is relevant to understanding ecosystem responses to water limitation because (*i*) allocation is known to vary considerably in response to environmental conditions (Malhi et al. 2011, Poorter et al. 2012, Franklin et al. 2012); and (*ii*) shifts in allocation can have important consequences for land surface processes (e.g., effects of leaf area on evapotranspiration; Zhang et al. 2001), C cycling (Farrior et al. 2015, Weng et al. 2015), and the vulnerability of species and ecosystems to drought (Kozlowski and Pallardy 2002).

Our study aims to address the following questions in an ESM context: Firstly, how does water limitation affect tree C allocation to fine roots, leaves, and wood for competitively dominant trees vs. those that maximize biomass, productivity, or drought-tolerance in monoculture? Secondly, how do allocational trait shifts, driven by competition, affect the responses of forest biomass and productivity to water stress? To explore the robustness of our results, we (*i*) explore the sensitivity of model outcomes to the assumed sensitivity of tree

mortality to water deficit, (*ii*) replicate our experiments with two sets of vegetation parameters, representing early- and late-successional tree types, and (*iii*) replicate our experiments with LM3-PPA and two versions of BiomeE (baseline and calibrated).

METHODS

We first describe the LM3-PPA model and the design of the main LM3-PPA experiments. Near the end of Methods, we describe alternative parameter sets and the BiomeE experiments used to evaluate the robustness of our results.

Summary of LM3-PPA model

LM3-PPA (Weng et al. 2015) is a demography-based DGVM – or 'vegetation demographic model' (VDM; Fisher et al. 2018) − in which the demographic rates (growth, mortality, and reproduction) of tree cohorts depend on resource competition. LM3-PPA was designed as an ESM component and represents land-atmosphere feedbacks on sub-daily time-scales (30-60 minutes, depending on the configuration). The LM3-PPA approach was incorporated into the terrestrial component of the GFDL Earth system model ESM4.1 (Dunne et al. 2020). In LM3-PPA, the distribution of 'plant strategies' (trait combinations representing different PFTs, species, etc.) across time and space is an emergent property of competition and the resulting demographic rates (Weng et al. 2015). Some model versions include competition for nitrogen (Weng et al. 2017) and other updates (Martínez Cano et al. 2020), but the present study only considers competition for light and water and is based on the original model version (Weng et al. 2015). LM3-PPA can be configured with different numbers of competing plant strategies. By incorporating individual-level processes and allowing for flexibility in the representation of plant functional diversity, LM3-PPA (like some other VDMs that are designed as ESM components;

e.g., Koven et al. 2020) offers the potential for improved representation of ecological processes in ESMs.

LM3-PPA is a deterministic (non-stochastic) model. A cohort in LM3-PPA is defined by (*i*) the properties of an individual tree (trait values, diameter, height, C pool sizes, etc.; these properties are assumed identical among individuals in a cohort) and (*ii*) its spatial density (number of trees per-unit ground area, which declines over time due to mortality). The dynamics are described by a system of size-structured partial differential equations (Strigul et al. 2008), with time-varying demographic rates that depend on meteorology, short time-scale physiological and biophysical processes, and competition (Weng et al. 2015).

LM3-PPA uses the Perfect Plasticity Approximation (PPA) space-filling algorithm to assign cohorts to one or more vertical canopy layers, with taller layers casting shade on shorter layers (Strigul et al. 2008). Radiation transfer in LM3-PPA is a multi-layer version of LM3's two-stream approximation for a single canopy layer (Meador and Weaver 1980). Competition for water occurs within and among all cohorts that are water-limited (i.e., cohorts whose water demand exceeds their supply at a given time), because all individuals (as represented by cohort densities) reduce the water supply available to other individuals. Plant water uptake in LM3-PPA depends on a cohort's fine-root surface area relative to competing cohorts in different soil layers. Each cohort's fine-root density is assumed to decay exponentially with soil depth, but roots are assumed to be horizontally well-mixed, so that all individuals compete for a common pool of water at a given depth. Photosynthesis and stomatal conductance are first calculated assuming abundant soil water (Farquhar et al. 1980, Collatz et al. 1991, Leuning 1995). If the resulting leaf-level demand for water is less than a cohort's water supply, then its photosynthesis and stomatal conductance are reduced accordingly.

Net C gain (photosynthesis minus respiration) is allocated on a half-daily time-step among different pools in the following priority order: leaves and fine roots (which are maintained in balance with each other and with sapwood cross-sectional area according to the pipe model; Shinozaki et al. 1964), nonstructural carbohydrates (NSCs), and sapwood and seeds. Trees allocate NSCs to fine roots and leaves until their targets (per-unit crown area) are met, and additional available C (in excess of a size- and strategy-specific NSC storage target) is allocated to sapwood and seeds in a 9:1 ratio (canopy trees) or only to sapwood (understory trees). Thus, sapwood allocation (wood production) depends on leaf, fine-root, and NSC targets, as well as environmental conditions that affect plant C balance (e.g., meteorology and the effects of competing trees on resource availability). Sapwood allocation, in turn, determines stem radial growth, height growth, and crown area following allometric relationships, and sapwood is converted to non-living heartwood to maintain constant ratios between sapwood cross-sectional area and fine-root and leaf surface areas. For the cold-deciduous trees considered in this study, fine roots and leaves are initiated/shed at the beginning/end of each growing season, which is determined by temperature thresholds. In this implementation of LM3-PPA, fine roots and leaves are not shed during the growing season (e.g., as a drought response) but may remain below their target values for an entire growing season depending on environmental conditions and resource competition.

Reproduction and mortality occur at the end of each year; as noted above, these are deterministic (non-stochastic) processes. Recruitment occurs via initiation of new seedling cohorts, whose densities depend on reproductive rates of canopy cohorts of the same strategy. Mortality is represented by the reduction in density of a cohort. Mortality occurs at a background rate (which differs among strategies and canopy layers) and if NSCs are completely depleted. In

this study, we also implemented a new mortality algorithm based on a cohort's cumulative water deficit (see below).

Overview of model experiments

This section provides an overview of LM3-PPA experiments. Details are presented in subsequent sections. Terms and abbreviations used frequently in the text are defined in Table 1.

We studied the performance of different allocational strategies in monoculture (single-strategy) and multi-strategy experiments under different precipitation and mortality scenarios. Multi-strategy experiments were designed to identify competitively dominant allocational strategies, which may differ from strategies that maximize biomass, productivity, or other aspects of performance in monoculture (i.e., in the absence of competition with other strategies). All experiments (monoculture and multi-strategy) include competition within and among multiple cohorts, whose size distribution reflects the demographic outcome of growth, mortality, and reproduction.

Results presented in the main text are based on simulations run to quasi-equilibrium with allocational variants of the late-successional tree species *Acer saccharum*. The variants differed in their allocation to leaves and fine roots (Fig. 1; with remaining available carbon allocated first to NSCs, and then to wood and reproduction), holding all other traits constant (e.g., wood density, allometry, photosynthetic and respiration parameters, and background mortality rates; Table S1). To assess the robustness of the results, we performed the following additional experiments: (*i*) the *Acer* experiments were repeated with allocational variants of the early-successional tree species *Populus tremuloides* (Table S1); and (*ii*) LM3-PPA experiments were

repeated with uncalibrated and empirically-calibrated versions of the BiomeE model (Weng et al. 2019), a computationally efficient analog for LM3-PPA.

All experiments were replicated using climate data from 10 grid cells (1° latitude × 1° longitude; hereafter 'sites') in the eastern USA (Fig. S1) under nine scenarios that combined three precipitation scenarios (dry, baseline, and wet) with three mortality assumptions (low, medium, and high sensitivity of tree mortality to water deficit). The 10 sites were selected to span temperature and precipitation gradients within the region of the USA dominated by deciduous broadleaved forests, which includes the Willow Creek, Wisconsin site where this version of LM3-PPA was tested (Weng et al. 2015). The 10 sites were also selected based on the availability of evaluation data (see 'Model-data comparisons' below). In our model experiments, the sites were assumed identical with respect to soil physical properties. We did not calibrate LM3-PPA vegetation parameters; except where noted (Table S1), we used parameter values reported by Weng et al. (2015) for Willow Creek. Thus, in our study, the 10 sites differ only with respect to climate. Our simulations have no explicit spatial scale (because the model tracks the spatial density of cohorts, rather than individuals *per se*) but should be interpreted as representing at least one hectare per site (the scale of PPA model tests; Strigul et al. 2008).

For each set of conditions (10 sites × 3 precipitation scenarios × 3 mortality scenarios; scenarios are described below), we identified the most competitive allocational strategy, as well as strategies that maximized different aspects of performance in monoculture (biomass, productivity, or drought-tolerance). Based on previous work with LM3-PPA (Weng et al. 2015, 2017) and simpler analogs (Dybzinski et al. 2011, 2015, Farrior et al. 2013, 2015, Weng et al. 2019), and given the absence of within-site edaphic heterogeneity or periodic large disturbances in our simulations, we expected that each set of conditions would lead to a single competitively

dominant (evolutionarily stable) strategy at equilibrium. Previous work shows that large disturbances permit tree species with different successional and spatial (e.g., edaphic) niches to coexist in the PPA model framework (Lichstein and Pacala 2011), but these forms of heterogeneity were not represented in our experiments. Thus, our multi-strategy experiments were not designed to study coexistence, but rather to explore what strategies would emerge as the competitive dominants under different conditions, assuming a diverse pool of strategies from which competition can select.

Trait variation

We explored variation in two allocational traits: target leaf area per crown area (LAI_{max}) and the ratio between fine-root surface area and leaf area ('root:leaf ratio', φ_{RL}). These two traits (LAI_{max} and φ_{RL}), combined with a tree's C balance, determine allocation to wood and reproduction (see 'Summary of LM3-PPA Model' above). The NSC target was assumed proportional to the sum of the leaf and fine-root targets. We defined 30 allocational strategies in the 2-dimensional leaf-root trait space (Fig. 1a), with the ranges for LAI_{max} (1 to 5), and φ_{RL} (0.5 to 3) chosen (based on preliminary experiments) to span the competitive and maximizing values across the experimental conditions. A given allocational strategy, along with other vegetation parameters (Table S1), determines individual rates of growth, mortality, and reproduction under different abiotic and competitive conditions (the sizes, densities, and traits of competing trees). The root:leaf ratio axis can also be viewed in terms of fine-root surface-area per crown-area (RAI_{max}; Fig. 1b), where $RAI_{max} = LAI_{max} \times \varphi_{RL}$. Each strategy in our experiments has fixed LAI and RAI targets (LAI_{max} and RAI_{max}, respectively), but LAI and RAI may fail to reach these targets if there is insufficient available C (see 'Summary of LM3-PPA Model' above).

Our exploration of allocational trait space focused on canopy trees, which have greater water demand than understory trees. For simplicity, we limited our exploration of understory traits to the following three cases: (*i*) understory LAI_{max} and φ_{RL} assumed equal to the corresponding canopy values for a given strategy; (*ii*) all understory trees assumed to have $LAI_{max} = 0.5$ and $\varphi_{RL} = 0.5$; and (*iii*) all understory trees assumed to have $LAI_{max} = 1$ and $\varphi_{RL} = 0.5$. In the trait space we explored (Fig. 1a), 0.5 is the smallest value of the root:leaf ratio (φ_{RL}); thus, cases *ii* and *iii* are consistent with the observation that the root:leaf ratio increases with irradiance (Poorter et al. 2012). Preliminary analyses suggested that all three cases led to qualitatively similar conclusions about canopy tree allocation strategies (the focus of this paper). We report results for case *iii*.

Precipitation scenarios

We used the Sheffield et al. (2006) 3-hourly, 1°-spatial reconstruction of historical climate (1948-2010) for the baseline precipitation scenario at each of the 10 sites (Fig. S1). We recycled the historical climate data as needed for long-term simulations. At each site, we defined 'dry' and 'wet' scenarios by multiplying each 3-hourly baseline precipitation value by 0.5 and 1.5, respectively. For simplicity, we did not adjust temperature or other meteorological variables when creating the dry and wet precipitation scenarios. Thus, these scenarios should be viewed as experimental conditions, rather than realistic climate scenarios.

Mortality scenarios

For each site and precipitation scenario, we considered three assumptions for tree mortality rate (μ; yr^{-1}) using the functional form:

$$\mu = \mu_0 + \frac{0.5-\mu_0}{1+e^{-20d+a}} \quad (1)$$

where *d* is the ratio of cumulative water deficit (the sum over a growing season of hourly water demand minus water supply; set to zero if supply exceeds demand) to cumulative water demand in a given growing season, and thus ranges from 0 to 1; μ_0 is the background mortality rate (Table S1); and parameter *a*, which determines the direct effect of water deficit on mortality, was set to +∞ (no direct response of mortality to water deficit), 15 (medium sensitivity), or 10 (high sensitivity) (Fig. 2). In addition to the direct effects of water deficit described by Eq. 1, mortality occurs if NSCs are completely depleted (C starvation), which can occur due to prolonged water deficit or shading. The direct role of water deficit in Eq. 1 follows Anderegg et al. (2012), who proposed that cumulative water deficit could serve as a useful proxy that integrates multiple physiological mechanisms related to drought-induced tree mortality, such as xylem cavitation. Eq. 1 could be fit to mortality data by embedding LM3-PPA in a data assimilation system (Raupach et al. 2005), but this approach is beyond the scope of our study. Because background mortality rates (μ_0; Table S1) were derived from forest inventories that capture all sources of mortality (including drought), the elevated mortality rates in the medium and high sensitivity cases (Fig. 2) are higher than observed mortality rates. Thus, our mortality scenarios should be viewed as an exploration of how different mortality assumptions affect tree C allocation, rather than an attempt to produce quantitatively accurate output.

Long-term experiments under stable climate

For each set of conditions (10 sites × 3 precipitation scenarios × 3 mortality scenarios), we identified the best-performing strategies (trait combinations; Fig. 1) in monoculture and in competition with other strategies. The dry, baseline, or wet climate (derived from the 1948-2010

climate data) was recycled for the duration of each experiment, and atmospheric CO_2 was held constant at the pre-industrial level (286 ppm). Thus, each long-term experiment included realistic levels of climate variability but no change in CO_2 or long-term climate.

We evaluated the performance of allocational strategies at quasi-equilibrium (as defined below). All simulations were initialized with a total density of 1500 seedlings ha^{-1}, but the quasi-equilibrium results should not be sensitive to the initial condition. The most competitive strategy (S_{COMP}; Table 1) was defined as the variant that produced the highest biomass in competition with other variants (see 'Identifying the competitively dominant strategy' below). In addition to S_{COMP}, we also identified the biomass-maximizing (S_{AGB}) and NPP-maximizing (S_{NPP}) strategies by simulating each of the 30 variants in monoculture. Other optimal monoculture strategies could be defined, such as the wood-growth-maximizing strategy (which was included in the BiomeE experiments described below). S_{AGB} and S_{NPP} were selected because they maximize important aspects of ecosystem functioning and may illustrate different behaviors relevant to optimality hypotheses. For example, because S_{NPP} maximizes total NPP (a large fraction of which may be allocated to fine roots and leaves that contribute little to standing biomass), S_{AGB} and S_{NPP} may differ substantially from each other. All LM3-PPA simulations used to evaluate S_{COMP}, S_{AGB}, and S_{NPP} lasted 500 years, which was sufficient to reach quasi-equilibrium (little or no trend in AGB or NPP during years 401-500). Accordingly, S_{COMP}, S_{AGB}, and S_{NPP} were identified based on mean AGB and NPP over years 401-500.

Identifying the competitively dominant strategy

Due to LM3-PPA's computational costs (largely due to the complex radiation and energy-balance calculations, which were performed on a 1-hour time-step in our implementation) and its

parallel computing architecture (designed for ESM experiments with many grid cells, but not optimized for site-level experiments as in the present study), we did not simulate polycultures with all 30 strategies competing simultaneously. Rather, we identified the competitively dominant strategy (S_{COMP}) by simulating all pairwise contests among the 30 strategies, as these could be distributed across different computer processors. For each case (10 sites × 3 precipitation scenarios × 3 mortality scenarios), there are 30×29/2 = 435 pairwise contests, with each of the 30 strategies competing in 29 contests. In all cases, the outcome of these pairwise contests indicated a clear S_{COMP}; i.e., a single strategy that won all 29 of its contests, where the winner of each contest was considered the variant with the higher AGB at quasi-equilibrium. Pairwise contests were initialized with 750 seedlings ha^{-1} per variant (total initial density of 1500 seedlings ha^{-1}), although the quasi-equilibrium results should not be sensitive to the initial conditions.

Although a clear S_{COMP} emerged from each set of pairwise contests, competitive exclusion did not always occur. Averaged across all pairwise contests, S_{COMP} comprised 94% of community (two-strategy) AGB during the quasi-equilibrium observation period (years 401-500). Simpler analogs of LM3-PPA have been shown to have a single evolutionarily stable strategy (ESS) under a given set of environmental conditions (Dybzinski et al. 2011, Farrior et al. 2013, 2015). It is possible that long-term stable coexistence is enabled by processes in LM3-PPA that are not represented in simpler models and/or by trends and variability in the 1948-2010 recycled climate data, but we have not explored coexistence in detail. We interpret each S_{COMP} as the single competitively dominant strategy for a given site and scenario, but we acknowledge that this interpretation may be incorrect in some cases, either because a single ESS does not exist, or because our 500-year experiments were not long enough to identify the correct ESS. A

looser interpretation of S_{COMP} is that it is one of potentially several competitive dominants for each site and scenario.

Novel drought experiments

To explore how allocational strategies affected drought tolerance, we subjected each variant to an extreme drought as follows: After each long-term (500-year) monoculture simulation, we simulated a five-year drought during which precipitation was reduced by 50% at every model time-step (no other forcing data were modified). Thus, at each site, drought was defined relative to the precipitation regime (dry, baseline, or wet scenario) over the preceding 500 years. We defined the most drought-tolerant strategy (S_{DT}) as the strategy with the highest AGB during the final (fifth) year of drought. We used this definition of drought tolerance because alternative definitions (e.g., based on the ratio or difference between post- and pre-drought AGB) strongly favored strategies with very low pre-drought AGB and did not always yield meaningful results. In addition to five-year drought, we also explored drought lengths up to 20 years. These longer periods led to qualitatively similar results; we only report results for five-year drought.

Quantifying biomass and productivity

For all analyses, biomass was defined as the maximum aboveground wood biomass (AGB; kg C m^{-2}) that occurred in a given year, and productivity was measured as cumulative net primary production (NPP; kg C m^{-2} yr^{-1}) for a given year. Defining biomass as total wood biomass (belowground plus aboveground) should lead to qualitatively similar results, because coarse root biomass is assumed to be a fixed fraction (20%) of total wood biomass in LM3-PPA and in the BiomeE model described below.

Model-data comparisons

Although the main goals of our study are to gain conceptual insights, rather than empirical applications with calibrated parameter values, we performed simple model-data comparisons to evaluate if LM3-PPA captured biomass and productivity trends across the 10 sites used for model experiments (Fig. S1). We compared empirical estimates of GPP, NPP, and AGB to LM3-PPA output at the 10 sites. For these comparisons, model simulations used the baseline climate data (1948-2010 recycled) and soil parameters (assumed constant across sites) used in other model experiments; soil parameters are for the Willow Creek site in Weng et al. (2015). The 10 sites used in these comparisons and in other model experiments were randomly selected from 1° latitude × 1° longitude grid cells in the USA that met the following criteria: (*i*) north of 35° latitude, (*ii*) east of -95° longitude, and (*iii*) at least 50 km^2 of mature forest (≥ 100 years old as of 2006) according to (Pan et al. 2011b). The mature-forest criterion was intended to minimize complications in model-data comparisons due to disturbance history. All model-data comparisons were based on simulated 101-110 year-old *Acer* forest and empirical estimates of GPP, NPP, and AGB for 101-110 year-old forest derived from MODIS satellite data (Running and Zhao 2015) and Forest Inventory and Analysis data (https://www.fia.fs.fed.us/) within 1° grid cells. For these comparisons, we present simulations for each of three *Acer* strategies identified in our long-term experiments at each site (S_{COMP}, S_{AGB}, and S_{NPP}). Predictions for S_{COMP}, S_{AGB}, and S_{NPP} used in the model-data comparisons are averaged over simulation years 101-110, and thus differ from quasi-equilibrium values (averaged over years 401-500) used in other analyses. Additional methods details for the model-data comparisons are presented in the Fig. S2 caption.

Alternative vegetation parameter values

To evaluate if our results were sensitive to vegetation parameter values, we repeated the long-term and novel-drought experiments described above (based on parameters values for the late-successional *Acer* species) using parameter values for an early-successional tree species, *Populus tremuloides* (Table S1). Wet scenarios for *Populus* were the same as for *Acer* (1.5 × baseline precipitation), but dry scenarios differed (0.8 × baseline for *Populus* compared to 0.5 × baseline for *Acer*), because at some sites, no *Populus* strategies were viable under 0.5, 0.6, or 0.7 × baseline precipitation.

Experiments with the BiomeE model

To further evaluate the robustness of our results, we replicated the LM3-PPA experiments for both *Acer* and *Populus* with the BiomeE model (Weng et al. 2019). BiomeE shares key features with LM3-PPA that are relevant to our study, including deterministic (non-stochastic) cohort demography, PPA-based height structured competition for light, and allocation-dependent competition for water. BiomeE was designed as a stand-alone ecosystem model, rather than an ESM component, and its representations of radiation transfer, energy flux, and hydrology are therefore simplified, resulting in execution times ~100 times faster than LM3-PPA. In the context of our study, we expect the most important difference between LM3-PPA and BiomeE to be soil hydrology. Following Weng et al. (2015), we configured LM3-PPA with a soil depth of 10 m subdivided into 20 layers ranging in depth from 2 cm (top layer) to 1 m (bottom layer). BiomeE uses the multi-layer bucket model approach from the TECO model (Weng and Luo 2008), here configured with 5 layers and a total depth of 3 m. The BiomeE bucket model has no

drainage from the bottom layer (Weng and Luo 2008, Weng et al. 2019), which should generally retain more water at depths accessible to roots compared to LM3-PPA.

For each site and scenario, we performed monoculture and polyculture experiments with BiomeE to identify S_{COMP}, S_{AGB}, S_{NPP}, and S_{DT} (Table 1), as well as the strategy that maximized the mean rate of wood production (S_{NPPw}) during the quasi-equilibrium observation period (final 100 simulation years). In many cases, we would expect S_{NPPw} to be similar to S_{AGB}, but these strategies may differ because S_{AGB} depends not only on wood production but also mortality (which can vary among strategies due to differences in water deficit). We used the same experimental protocols for BiomeE and LM3-PPA except that rather than identifying S_{COMP} using pairwise contests (as with LM3-PPA), we used polyculture experiments with all 30 strategies competing simultaneously to identify S_{COMP} in BiomeE. These polycultures (initialized with 50 seedlings ha^{-1} per variant, for a total initial seedling density of 1500 ha^{-1}) were simulated for 1244 years, with the final 100 years serving as the observation period for identifying S_{COMP} (the strategy with the highest quasi-equilibrium AGB in polyculture). Averaged across all BiomeE polyculture simulations, S_{COMP} comprised 69% of community AGB during the quasi-equilibrium observation period (70% and 68%, respectively, for the uncalibrated and calibrated BiomeE versions described below). In some cases, a single strategy competitively excluded all others, whereas in other cases, several strategies had similar AGB at the end of the 1244-year simulation. As explained for LM3-PPA above, we do not know if these apparent coexistence cases indicate stable long-term coexistence. We assume that each S_{COMP} identified by our methodology is either the single ESS or is one of several competitively dominant strategies.

To evaluate potential consequences of model-data mismatches, we present results from both uncalibrated and empirically-calibrated BiomeE versions (empirical estimates are described in 'Model-data comparisons' above and Fig. S2). The uncalibrated BiomeE version had the same values for key vegetation parameters as LM3-PPA (Table S1) except for slightly higher values of the V_{cmax} photosynthetic parameter (Table S2). We calibrated BiomeE by repeating the experiments while tuning V_{cmax} and respiration per-unit sapwood area (β_{sw}) to achieve a close match to empirical estimates of GPP and NPP (Table S2).

RESULTS

Model-data comparisons

Empirical estimates of GPP, NPP, and AGB in 101-110 year-old forest were highly variable within each 1° grid cell, but tended to increase with both mean annual temperature and precipitation across the 10 sites (Fig. S2: error bars show the central 95% of empirical estimates within grid cells). For LM3-PPA, the three strategies used in the model-data comparisons (S_{COMP}, S_{AGB}, and S_{NPP}; Table 1) yielded GPP, NPP, and AGB predictions in 101-110 year-old forest that were lower than empirical means (Table S2) but tended to increase with temperature and precipitation across the 10 sites in a similar manner as the empirical estimates (Fig. S2). S_{COMP}, S_{AGB}, and S_{NPP} yielded similar predictions to each other at most sites for 101-110 year-old forest, but differed by up to a factor of ~2 in some cases (Fig. S2).

In contrast to LM3-PPA, the uncalibrated BiomeE model yielded predictions of GPP, NPP, and AGB that were higher than empirical means (Fig. S3 and Table S2). Tuning two physiological parameters (V_{cmax} and β_{sw}) allowed for a close match between BiomeE predictions

and empirical estimates of GPP and NPP, but predicted AGB remained higher than empirical estimates (Fig. S4 and Table S2).

Effects of water limitation on tree C allocation

Increasing water stress (shift from wet to dry climate, and increasing mortality sensitivity to water deficit) led to lower leaf-area targets (LAI_{max}) and/or higher root:leaf ratios (φ_{RL}) for competitive and maximizing strategies in most cases (Figs. 3 and S5-S9). These trends were clearer in LM3-PPA (where the identified strategies were typically in the interior of the explored trait space; Figs. 3 and S5) compared to BiomeE (where the identified strategies were sometimes at the edge of the explored trait space; Figs. S6-S9). Nevertheless, trends towards lower LAI_{max} and/or higher φ_{RL} with increasing water stress usually occurred in LM3-PPA and in both uncalibrated and calibrated BiomeE versions. The main exception to these trends occurred for the productivity-maximizing strategy (S_{NPP}) in BiomeE, whose φ_{RL} was often highest under wet climate (Figs. S6-S9).

Increasing water stress tended to cause smaller decreases in LAI_{max} and larger increases in φ_{RL} for competitive than for maximizing strategies (Figs. 3 and S5-S9). Therefore, relative to S_{COMP}, maximizing values of LAI_{max} and φ_{RL} tended to decrease with increasing water stress (Figs. 4 and S10-S14; equivalently, relative to maximizing strategies, competitive LAI_{max} and φ_{RL} tended to increase with increasing water stress). These trends were generally robust, with the main exception occurring for LM3-PPA *Populus* experiments with high mortality (Fig. S10g-i).

The most drought-tolerant strategy (S_{DT}; here defined as the strategy that maintains the highest biomass following novel drought) had low LAI_{max} compared to other strategies (Figs. 3 and S5-S9). S_{DT} was often similar to strategies that maximized biomass (S_{AGB}) and wood

production (S_{NPPw}) but markedly differed from S_{COMP} and S_{NPP}, particularly under dry climate and/or high mortality scenarios (Figs. 3 and S5-S9).

Effects of trait shifts on ecosystem responses to climate change

Changing environmental conditions across space or time are expected to result in shifts in the competitively dominant strategy, which we refer to as 'trait shifts' following Sakschewski et al. (2016). The effects of trait shifts can be evaluated by comparing the climate responses of AGB and NPP that result from S_{COMP} shifts (dashed lines in Figs. 5 and S15-S19) to the responses that would emerge from fixed competitive strategies (colored symbols in Figs. 5 and S15-S19).

For *Acer*, trait shifts from wet to dry climates led to non-linear decreases in AGB and NPP (dashed lines in Figs. 5, S16, and S18). In most cases, these climate responses were similar to those of the baseline and wet fixed strategies ($S_{COMPbaseline}$ and $S_{COMPwet}$) but stronger than the climate response of the dry fixed strategy ($S_{COMPdry}$) due to its relatively low AGB and NPP under baseline and wet climates (Figs. 5, S16, and S18). For *Acer*, differences between LM3-PPA and BiomeE were most notable for the high mortality scenario: $S_{COMPbaseline}$ and $S_{COMPwet}$ had very low (sometimes zero) AGB and NPP under dry climate in LM3-PPA (Figs. 5e-f) but not in BiomeE (Figs. S16e-f and S18e-f). In contrast to *Acer*, trait shifts for *Populus* had weak ecosystem-level effects, because all three competitive *Populus* strategies had similar AGB and NPP across the three climate scenarios within a given model (Figs. S15, S17, and S19).

In summary, effects of allocational trait shifts depended strongly on non-allocational vegetation parameter values (*Acer* vs. *Populus*) and to a lesser extent on the model (LM3-PPA vs. BiomeE). Mean AGB and NPP differed between uncalibrated and calibrated BiomeE versions, but the two versions yielded similar climate responses (Figs. S16-S19).

DISCUSSION

Competitive vs. maximizing allocation strategies under water limitation

In our study, competitively dominant allocation strategies diverged from those that maximize biomass or productivity, which highlights a potential challenge in applying optimality principles to improving vegetation and climate models (Harrison et al. 2021). Competitive and maximizing strategies are expected to be equivalent for traits whose effects on fitness do not depend on the strategies of neighbors (Harrison et al. 2021); potential examples include leaf carboxylation capacity (V_{cmax}) (Wang et al. 2017) and leaf nitrogen content (Caldararu et al. 2020). However, if the root systems of neighboring plants overlap – as appears common (Hodgkins and Nichols 1977, Casper et al. 2003, Göttlicher et al. 2008) – then an individual's access to belowground resources will depend not only on its own traits but also those of its neighbors, allowing for the possibility of competitive arms races. Under these conditions, competitive and maximizing strategies are expected to diverge, as observed in our study (where roots are assumed to be horizontally well-mixed) and in previous theoretical and empirical studies (e.g., King 1993, Gersani et al. 2001, Craine 2006, Dybzinski et al. 2011, Franklin et al. 2012, Farrior et al. 2013, 2015, Wolf et al. 2016, Anderegg et al. 2018).

Our experiments with LM3-PPA – a vegetation demographic model (VDM; Fisher et al. 2018) designed as an Earth system model (ESM) component – suggest that as water stress becomes more severe, competitive strategies increase their allocation to fine roots and leaves relative to maximizing strategies; i.e., LM3-PPA predicts a 'competitive overinvestment' in both fine roots and leaves for water-limited plants. In absolute terms, competitive strategies (S_{COMP}) are predicted to reduce their leaf area with increasing water stress, but less so than maximizing

strategies; therefore, S_{COMP} becomes leafier relative to maximizing strategies with increasing water stress. The competitive overinvestment in fine roots predicted by LM3-PPA is consistent with potted plant experiments and predictions from multiple models (Gersani et al. 2001, Franklin et al. 2012, Farrior et al. 2013, 2015). In contrast, the competitive overinvestment in leaf area predicted by LM3-PPA under dry conditions has not, to our knowledge, previously been discussed in the literature but is predicted by the model of Farrior et al. (2015; compare leaf NPP in their Figs. 2 and S4.1).

Competitive overinvestment in leaf area appears to depend on transient soil-moisture dynamics and/or effects of plant traits on community-level water uptake (i.e., water not lost to evaporation, drainage, or runoff). These processes are represented in many vegetation models – including the LM3-PPA and BiomeE models studied here and in Farrior et al. (2015) – but not in the simpler model of Farrior et al. (2013), which predicts convergent leaf allocation (but divergent root allocation) for competitive and maximizing strategies. Below, we suggest two non-mutually exclusive mechanisms that may explain competitive overinvestment in leaf area.

The first mechanism that may explain competitive overinvestment in leaf area relates to transient soil-moisture dynamics. In a temporally variable environment, time-averaged ecosystem-level productivity may be maximized by limiting leaf area to a level that is suboptimal during wet periods in order to save soil water for subsequent dry periods (when the marginal benefit of additional water should be large). While this efficient strategy may maximize time-averaged productivity, it is prone to invasion by strategies that spend (rather than save) water in the short term if doing so provides a competitive advantage (Cohen 1970, Wolf et al. 2016). In a temporally variable environment, a competitive strategy may be to maintain sufficient leaf area to maximize productivity and water use during wet periods, which would

increase the time span and degree of water limitation, as well as the competitive advantage of high root allocation during dry periods.

The second mechanism that may explain competitive overinvestment in leaf area relates to hydrological losses (evaporation, drainage, and runoff). Competitive plants overinvest in fine roots and are thus relatively effective in mining soil water and preventing hydrological losses. Theory suggests that the resulting increase in water supply should lead to increased leaf area up to the point where self-shading or other factors reduce net C gains to zero (Farrior et al. 2015; see their Table S3.1). This prediction, which assumes fixed annual leaf-building costs and does not apply to time scales shorter than a growing season, is best interpreted as the most competitive fixed leaf strategy (LAI target) for a given root strategy and hydrological regime.

The generality of competitive overinvestments in roots and leaves could be explored in future studies using experiments with models (beyond those studied here) and/or model-data comparisons. Competitive overinvestment in roots should occur if, during periods of water limitation, a plant's water supply increases with its root investment relative to neighboring plants (Farrior et al. 2013). The conditions leading to competitive overinvestment in leaves are less well understood, but we hypothesize that it emerges from a competitive overinvestment in roots along with one or both of the hydrological mechanisms proposed above. Model experiments could be designed to better understand the conditions leading to competitive overinvestment in leaves. In terms of empirical tests of the predicted overinvestments, the most practical approach may be to compare predictions from different model versions (competitive vs. maximizing traits) to observations of LAI and fluxes of C and water. An effective implementation of this approach would require more rigorous estimation of soil and plant physiological parameters than in the present study.

Consequences of competitive allocation for forest biomass and productivity

Given that high belowground allocation is both a potential drought-avoidance strategy (Poorter et al. 2012) and a competitive strategy when water or nutrients are limiting (e.g., King 1993, Gersani et al. 2001, Craine 2006, Dybzinski et al. 2011, Farrior et al. 2013), we expected S_{COMP} to perform well under novel drought. S_{COMP} was often similar to the most drought-tolerant strategy (S_{DT}) under baseline and wet climates. However, a dry climate combined with novel drought often resulted in S_{COMP} having substantially lower biomass and productivity than S_{DT} (results not shown). The competitive overinvestment in leaf area likely makes S_{COMP} vulnerable to novel drought, particularly in a dry climate.

Climate-driven shifts in S_{COMP} ('trait shifts') led to greater resilience and ecosystem functioning in some cases we studied. In LM3-PPA experiments, strategies that were most competitive under baseline and wet climate were sometimes inviable under dry climate, whereas trait shifts allowed for viable populations (Figs. 5 and S15). Also, in LM3-PPA *Acer* experiments, trait shifts led to higher mean AGB and NPP (averaged across climate scenarios) than any of the fixed competitive strategies (Fig. 5). These behaviors illustrate some possible outcomes of incorporating diversity, competition, and demography into ESMs but were not consistently observed across vegetation parameter sets (*Acer* and *Populus*) or the two models we studied (LM3-PPA and BiomeE). Variable ecosystem-level consequences of trait shifts have also been observed in previous studies. Trait shifts moderated biomass responses to climate change on centennial time-scales in a previous VDM study (Sakschewski et al. 2016). In contrast, on decadal time-scales, trait shifts had little impact in the same VDM study (Sakschewski et al. 2016) and amplified responses to climate variability in an empirical study of eastern USA forests

(Zhang et al. 2018). Amplified responses were also observed in previous work with LM3-PPA and BiomeE, which revealed that competition increases fine-root allocation in response to CO_2 fertilization (Weng et al. 2015) and that this allocational shift increases ecosystem sensitivity to nitrogen limitation (Weng et al. 2019). These studies indicate that trait shifts often lead to different ecosystem responses than fixed strategies but also highlight the variety of potential outcomes.

Robustness of results

Competitive overinvestment in roots and leaves under water-limited conditions was mostly consistent across a broad range of modeling contexts, including experiments based on parameter sets for early- and late-successional tree species (*Populus* and *Acer*, respectively), VDMs that differed in soil hydrology and biophysical complexity (LM3-PPA and BiomeE), and uncalibrated vs. calibrated BiomeE versions. Because BiomeE was designed as a computationally efficient analog for LM3-PPA, the two models are not independent. Experiments with other, independently derived models would help determine the generality of our results.

The computational expense of LM3-PPA simulations constrained some aspects of our experimental design, including the exploration of trait space (two dimensions that determined allocation to leaves, fine-roots, and wood), the lack of model calibration (systematic underprediction of GPP, NPP, and AGB relative to empirical estimates), and the use of pairwise contests to identify S_{COMP} among 30 allocational variants. Experiments with the BiomeE model (which executes ~100 times faster than LM3-PPA) suggest that the competitive overinvestments in roots and leaves predicted by LM3-PPA are qualitatively robust. These competitive overinvestments were observed in experiments with the baseline (uncalibrated) BiomeE version

as well as an empirically-calibrated version. For BiomeE, S_{COMP} was identified by competing all 30 variants simultaneously in polyculture. We did not perform controlled comparisons of the pairwise (LM3-PPA) and polyculture (BiomeE) S_{COMP} methods, but the broad agreement across models suggests that competitive overinvestment in roots and leaves is qualitatively robust to the method of identifying S_{COMP}.

Effects of trait shifts on ecosystem climate responses were less robust, depending strongly on vegetation parameter sets (*Acer* vs. *Populus*) and to a lesser extent on the choice of model, with trait-shift effects being somewhat stronger for LM3-PPA than for BiomeE (but similar between uncalibrated and calibrated BiomeE versions). Beyond the effects of trait shifts, the effects of allocation strategy (e.g., competitive vs. different maximizing strategies) on ecosystem biomass and productivity varied, in general, among the different modeling contexts we explored (results not shown). While competitive overinvestment of roots and leaves appears to be a robust result across a range of conditions, the effect of different allocational strategies on biomass and productivity appears to be more context dependent.

Limitations and future directions

The LM3-PPA and BiomeE versions used in our study consider competition for only water and light. Other model versions consider competition for nitrogen, which affects the geography of plant functional types as well as ecosystem responses to CO_2 fertilization (Weng et al. 2017, 2019). In our study, competitive strategies had relatively low allocation to fine roots and leaves (and thus high allocation to wood) under wet climate conditions. If nutrients were limiting in our simulations – as is often the case in reality (Vitousek and Howarth 1991, Vitousek et al. 2010) –

we would expect a competitive overinvestment in roots even in the absence of water limitation (King 1993, Craine 2006, Dybzinski et al. 2011).

In our experiments, increasing the assumed sensitivity of mortality to water deficit resulted in larger allocational shifts (for all strategy types) across climates, as well as a greater competitive overinvestment in roots and leaves, but did not lead to qualitatively different conclusions. Thus, insights from simpler models that lack this mortality mechanism (e.g., Dybzinski et al. 2011, 2015, Farrior et al. 2013, 2015) likely still apply to more complex models, even if the models diverge in their quantitative predictions. In our study, water-deficit-based mortality was added to the background mortality rate. A next step is to implement a model-data fusion framework (e.g., Raupach et al. 2005, Lichstein et al. 2014) to incorporate drought-dependent mortality while maintaining consistency with observed mortality rates.

Our results were derived from experiments that were run to quasi-equilibrium and which are therefore agnostic about the time scale of ecosystem responses and trait dynamics. For example, trait shifts driven by climate change (Fig. 5) can be conceptualized as resulting from local adaptation, shifting species composition, individual plasticity, or some combination thereof. The importance of incorporating trait plasticity into DGVMs is widely recognized (e.g., Wullschleger et al. 2014), and some DGVMs assume allocational plasticity in response to water limitation (Friedlingstein et al. 1999, Ostle et al. 2009, Zaehle and Friend 2010). However, identifying the most competitive plastic allocation strategy will be challenging. For example, the competitive benefit of shedding leaves during a drought depends on factors beyond the instantaneous effects on plant C balance, including the remaining length of the growing season (which affects the opportunity cost of leaf shedding) and the strategies of neighbors.

One approach to exploring plastic competitive allocation would be to define an allocational strategy as a set of response functions, rather than a set of fixed traits. For a given trait θ, these response functions, $\theta = f(\mathbf{x})$, would specify the trait value as a function of environmental variables, **x** (water deficit, atmospheric CO_2, etc.). This approach differs from current DGVM implementations of allocational plasticity in that multiple plastic strategies would be defined – $f_1(\mathbf{x})$, $f(\mathbf{x})_2$, …, $f_n(\mathbf{x})$ – and would then be subject to competitive and environmental filtering.

Finally, the exploration of trait space presented here is far from complete. We assumed uniform traits for understory trees while exploring a two-dimensional trait space for canopy trees. We have not yet explored understory allocation as additional axes of variation. In general, regeneration dynamics are a critical yet understudied aspect of ESMs (Hanbury-Brown et al. 2022). For both understory and canopy trees, trait dimensions other than those we studied can strongly affect vegetation response to water stress, including rooting depth, nonstructural carbohydrate storage, and hydraulic traits (McDowell et al. 2013, Christoffersen et al. 2016). However, systematically exploring different optimality concepts in a high-dimensional trait space – as we have done here in two dimensions – would be difficult for computationally demanding VDMs such as LM3-PPA that are designed as ESM components.

To move beyond experiments aimed at understanding model behavior, regional- to global-scale applications with VDMs will require efficient algorithms to explore trait spaces; e.g., to generate functional diversity that is then subject to competitive and environmental filtering (Franklin et al. 2020). A simple approach to generating trait diversity is to randomly sample new recruits from a pre-defined trait space (e.g., Sakschewski et al. 2016). Biologically, this pre-defined trait space represents the regional species pool; thus, this approach assumes, but

cannot explain, regional diversity (Franklin et al. 2020). Evolutionary algorithms (including crossover and mutation; Scheiter et al. 2013) provide an alternative, more biological approach to exploring high-dimensional trait spaces in VDMs. The representation of processes that create and maintain functional diversity in VDMs within grid cells and at broader geographic scales remains an important topic for future research (Fisher and Koven 2020). One promising direction is the implementation of fine-scale edaphic-topographic heterogeneity in ESMs (Zorzetto et al. 2023); when combined with metacommunity processes (Lichstein and Pacala 2011), this heterogeneity could maintain diversity across spatial scales.

Conclusions

Efforts to improve the representation of trait diversity in ESMs should consider potential differences among optimality concepts. Traits that are optimal with respect to ecosystem functioning or fitness components in monoculture (i.e., in the absence of interspecific competition) are not necessarily optimal from a competitive standpoint and thus may be unlikely to emerge from community assembly processes. Accurately representing competitive outcomes in ESMs will require either more general approaches to competitive optimization and/or explicitly modeling coexistence and community assembly. These approaches are not mutually exclusive. Well-supported optimality-based predictions could be used to represent variation in some trait dimensions, while explicitly modeling coexistence and community assembly may still be necessary to accurately represent variation in other dimensions where reliable predictions are not available.

Acknowledgements

Funding was provided by the USDA Forest Service Northern Research Station (agreements 09-JV-11242306-051, 13-JV-11242315-066, and 11-JV-11242306-059); the Princeton Environmental Institute; the National Oceanic and Atmospheric Administration (US Department of Commerce; grant NA08OAR4320752); the National Institute for Mathematical and Biological Synthesis (NSF Award DBI-1300426, with additional support from The University of Tennessee, Knoxville); and the NASA Modeling, Analysis, and Prediction (MAP) Program (grant 80NSSC21K1496).

Conflict of Interest Statement

The authors declare no conflict of interest.

Author contributions

Jeremy Lichstein and Tao Zhang designed the research. Tao Zhang ran the LM3-PPA simulations, and Ensheng Weng ran the BiomeE simulations. Tao Zhang analyzed model output. Jeremy Lichstein and Tao Zhang wrote the initial manuscript draft. All authors interpreted results and edited the manuscript.

Data availability

Model code and outputs are archived on Zenodo: https://doi.org/10.5281/zenodo.13376013 (Lichstein et al. 2024).

References

Anderegg, W. R. L., J. A. Berry, and C. B. Field. 2012. Linking definitions, mechanisms, and modeling of drought-induced tree death. Trends in Plant Science 17:693–700.

Anderegg, W. R. L., C. Schwalm, F. Biondi, J. J. Camarero, G. Koch, M. Litvak, K. Ogle, J. D. Shaw, E. Shevliakova, A. P. Williams, A. Wolf, E. Ziaco, and S. Pacala. 2015. Pervasive drought legacies in forest ecosystems and their implications for carbon cycle models. Science 349:528–532.

Anderegg, W. R. L., A. Wolf, A. Arango-Velez, B. Choat, D. J. Chmura, S. Jansen, T. Kolb, S. Li, F. C. Meinzer, P. Pita, V. Resco de Dios, J. S. Sperry, B. T. Wolfe, and S. Pacala. 2018. Woody plants optimise stomatal behaviour relative to hydraulic risk. Ecology Letters 21:968–977.

Arora, V. K., A. Katavouta, R. G. Williams, C. D. Jones, V. Brovkin, P. Friedlingstein, J. Schwinger, L. Bopp, O. Boucher, P. Cadule, M. A. Chamberlain, J. R. Christian, C. Delire, R. A. Fisher, T. Hajima, T. Ilyina, E. Joetzjer, M. Kawamiya, C. D. Koven, J. P. Krasting, R. M. Law, D. M. Lawrence, A. Lenton, K. Lindsay, J. Pongratz, T. Raddatz, R. Seferian, K. Tachiiri, J. F. Tjiputra, A. Wiltshire, T. Wu, and T. Ziehn. 2020. Carbon-concentration and carbon-climate feedbacks in CMIP6 models and their comparison to CMIP5 models. Biogeosciences 17:4173–4222.

Caldararu, S., T. Thum, L. Yu, and S. Zaehle. 2020. Whole-plant optimality predicts changes in leaf nitrogen under variable CO_2 and nutrient availability. New Phytologist 225:2331–2346.

Casper, B. B., H. J. Schenk, and R. B. Jackson. 2003. Defining a plant's belowground zone of influence. Ecology 84:2313–2321.

Christoffersen, B. O., M. Gloor, S. Fauset, N. M. Fyllas, D. R. Galbraith, T. R. Baker, B. Kruijt, L. Rowland, R. A. Fisher, O. J. Binks, S. Sevanto, C. Xu, S. Jansen, B. Choat, M. Mencuccini, N. G. McDowell, and P. Meir. 2016. Linking hydraulic traits to tropical forest function in a size-structured and trait-driven model (TFS v.1-Hydro). Geoscientific Model Development 9:4227–4255.

Cohen, D. 1970. The expected efficiency of water utilization in plants under different competition and selection regimes. Israel Journal of Botany 19:50–54.

Collatz, G. J., J. T. Ball, C. Grivet, and J. A. Berry. 1991. Physiological and environmental regulation of stomatal conductance, photosynthesis and transpiration: a model that includes a laminar boundary layer. Agricultural and Forest Meteorology 54:107–136.

Craine, J. M. 2006. Competition for nutrients and optimal root allocation. Plant and Soil 285:171–185.

Dantas de Paula, M., M. Forrest, L. Langan, J. Bendix, J. Homeier, A. Velescu, W. Wilcke, and T. Hickler. 2021. Nutrient cycling drives plant community trait assembly and ecosystem functioning in a tropical mountain biodiversity hotspot. New Phytologist 232:551–566.

Detto, M., J. M. Levine, and S. W. Pacala. 2022. Maintenance of high diversity in mechanistic forest dynamics models of competition for light. Ecological Monographs 92:e1500.

Dunne, J. P., L. W. Horowitz, A. J. Adcroft, P. Ginoux, I. M. Held, J. G. John, J. P. Krasting, S. Malyshev, V. Naik, F. Paulot, E. Shevliakova, C. A. Stock, N. Zadeh, V. Balaji, C. Blanton, K. A. Dunne, C. Dupuis, J. Durachta, R. Dussin, P. P. G. Gauthier, S. M. Griffies, H. Guo, R. W. Hallberg, M. Harrison, J. He, W. Hurlin, C. McHugh, R. Menzel, P. C. D. Milly, S. Nikonov, D. J. Paynter, J. Ploshay, A. Radhakrishnan, K. Rand, B. G. Reichl, T. Robinson, D. M. Schwarzkopf, L. T. Sentman, S. Underwood, H. Vahlenkamp, M. Winton, A. T. Wittenberg, B. Wyman, Y. Zeng, and M. Zhao. 2020. The GFDL Earth System Model Version 4.1 (GFDL-ESM 4.1): Overall Coupled Model Description and Simulation Characteristics. Journal of Advances in Modeling Earth Systems 12:e2019MS002015.

Dybzinski, R., C. E. Farrior, and S. W. Pacala. 2015. Increased forest carbon storage with increased atmospheric CO_2 despite nitrogen limitation: a game-theoretic allocation model for trees in competition for nitrogen and light. Global Change Biology 21:1182–1196.

Dybzinski, R., C. Farrior, A. Wolf, P. B. Reich, and S. W. Pacala. 2011. Evolutionarily stable strategy carbon allocation to foliage, wood, and fine roots in trees competing for light and nitrogen: an analytically tractable, individual-based model and quantitative comparisons to data. American Naturalist 177:153–166.

Falster, D. S., A. Braennstroem, M. Westoby, and U. Dieckmann. 2017. Multitrait successional forest dynamics enable diverse competitive coexistence. Proceedings of the National Academy of Sciences 114:E2719–E2728.

Farquhar, G. D., S. V. Caemmerer, and J. A. Berry. 1980. A biochemical model of photosynthetic CO_2 assimilation in leaves of C_3 species. Planta 149:78–90.

Farrior, C. E., R. Dybzinski, S. A. Levin, and S. W. Pacala. 2013. Competition for water and light in closed-canopy forests: a tractable model of carbon allocation with implications for carbon sinks. American Naturalist 181:314–330.

Farrior, C. E., I. Rodriguez-Iturbe, R. Dybzinski, S. A. Levin, and S. W. Pacala. 2015. Decreased water limitation under elevated CO_2 amplifies potential for forest carbon sinks. Proceedings of the National Academy of Sciences 112:7213–7218.

Fisher, R. A., and C. D. Koven. 2020. Perspectives on the Future of Land Surface Models and the Challenges of Representing Complex Terrestrial Systems. Journal of Advances in Modeling Earth Systems 12:e2018MS001453.

Fisher, R. A., C. D. Koven, W. R. L. Anderegg, B. O. Christoffersen, M. C. Dietze, C. E. Farrior, J. A. Holm, G. C. Hurtt, R. G. Knox, P. J. Lawrence, J. W. Lichstein, M. Longo, A. M. Matheny, D. Medvigy, H. C. Muller-Landau, T. L. Powell, S. P. Serbin, H. Sato, J. K. Shuman, B. Smith, A. T. Trugman, T. Viskari, H. Verbeeck, E. Weng, C. Xu, X. Xu, T. Zhang, and P. R. Moorcroft. 2018. Vegetation demographics in Earth System Models: A review of progress and priorities. Global Change Biology 24:35–54.

Fisher, R. A., S. Muszala, M. Verteinstein, P. Lawrence, C. Xu, N. G. McDowell, R. G. Knox, C. Koven, J. Holm, B. M. Rogers, A. Spessa, D. Lawrence, and G. Bonan. 2015. Taking off the training wheels: the properties of a dynamic vegetation model without climate envelopes, CLM4.5(ED). Geoscientific Model Development 8:3593–3619.

Franklin, O., S. P. Harrison, R. Dewar, C. E. Farrior, A. Braennstroem, U. Dieckmann, S. Pietsch, D. Falster, W. Cramer, M. Loreau, H. Wang, A. Makela, K. T. Rebel, E. Meron, S. J. Schymanski, E. Rovenskaya, B. D. Stocker, S. Zaehle, S. Manzoni, M. van Oijen, I. J. Wright, P. Ciais, P. M. van Bodegom, J. Penuelas, F. Hofhansl, C. Terrer, N. A. Soudzilovskaia, G. Midgley, and I. C. Prentice. 2020. Organizing principles for vegetation dynamics. Nature Plants 6:444–453.

Franklin, O., J. Johansson, R. C. Dewar, U. Dieckmann, R. E. McMurtrie, A. Brannstrom, and R. Dybzinski. 2012. Modeling carbon allocation in trees: a search for principles. Tree Physiology 32:648–666.

Friedlingstein, P., P. Cox, R. Betts, L. Bopp, W. Von Bloh, V. Brovkin, P. Cadule, S. Doney, M. Eby, I. Fung, G. Bala, J. John, C. Jones, F. Joos, T. Kato, M. Kawamiya, W. Knorr, K. Lindsay, H. D. Matthews, T. Raddatz, P. Rayner, C. Reick, E. Roeckner, K. G. Schnitzler, R. Schnur, K. Strassmann, A. J. Weaver, C. Yoshikawa, and N. Zeng. 2006. Climate-carbon cycle feedback analysis: Results from the C^4MIP model intercomparison. Journal of Climate 19:3337–3353.

Friedlingstein, P., G. Joel, C. B. Field, and I. Y. Fung. 1999. Toward an allocation scheme for global terrestrial carbon models. Global Change Biology 5:755–770.

Friedlingstein, P., M. O'Sullivan, M. W. Jones, R. M. Andrew, D. C. E. Bakker, J. Hauck, P. Landschützer, C. Le Quéré, I. T. Luijkx, G. P. Peters, W. Peters, J. Pongratz, C. Schwingshackl, S. Sitch, J. G. Canadell, P. Ciais, R. B. Jackson, S. R. Alin, P. Anthoni, L. Barbero, N. R. Bates, M. Becker, N. Bellouin, B. Decharme, L. Bopp, I. B. M. Brasika, P. Cadule, M. A. Chamberlain, N. Chandra, T.-T.-T. Chau, F. Chevallier, L. P. Chini, M. Cronin, X. Dou, K. Enyo, W. Evans, S. Falk, R. A. Feely, L. Feng, D. J. Ford, T. Gasser, J. Ghattas, T. Gkritzalis, G. Grassi, L. Gregor, N. Gruber, Ö. Gürses, I.

Harris, M. Hefner, J. Heinke, R. A. Houghton, G. C. Hurtt, Y. Iida, T. Ilyina, A. R. Jacobson, A. Jain, T. Jarníková, A. Jersild, F. Jiang, Z. Jin, F. Joos, E. Kato, R. F. Keeling, D. Kennedy, K. Klein Goldewijk, J. Knauer, J. I. Korsbakken, A. Körtzinger, X. Lan, N. Lefèvre, H. Li, J. Liu, Z. Liu, L. Ma, G. Marland, N. Mayot, P. C. McGuire, G. A. McKinley, G. Meyer, E. J. Morgan, D. R. Munro, S.-I. Nakaoka, Y. Niwa, K. M. O'Brien, A. Olsen, A. M. Omar, T. Ono, M. Paulsen, D. Pierrot, K. Pocock, B. Poulter, C. M. Powis, G. Rehder, L. Resplandy, E. Robertson, C. Rödenbeck, T. M. Rosan, J. Schwinger, R. Séférian, T. L. Smallman, S. M. Smith, R. Sospedra-Alfonso, Q. Sun, A. J. Sutton, C. Sweeney, S. Takao, P. P. Tans, H. Tian, B. Tilbrook, H. Tsujino, F. Tubiello, G. R. Van Der Werf, E. Van Ooijen, R. Wanninkhof, M. Watanabe, C. Wimart-Rousseau, D. Yang, X. Yang, W. Yuan, X. Yue, S. Zaehle, J. Zeng, and B. Zheng. 2023. Global Carbon Budget 2023. Earth System Science Data 15:5301–5369.

Friend, A. D., A. K. Stevens, R. G. Knox, and M. G. R. Cannell. 1997. A process-based, terrestrial biosphere model of ecosystem dynamics (Hybrid v3.0). Ecological Modelling 95:249–287.

Gersani, M., J. S. Brown, E. E. O'Brien, G. M. Maina, and Z. Abramsky. 2001. Tragedy of the commons as a result of root competition. Journal of Ecology 89:660–669.

Göttlicher, S. G., A. F. S. Taylor, H. Grip, N. R. Betson, E. Valinger, M. N. Hogberg, and P. Hogberg. 2008. The lateral spread of tree root systems in boreal forests:: Estimates based on ¹⁵N uptake and distribution of sporocarps of ectomycorrhizal fungi. Forest Ecology and Management 255:75–81.

Gravel, D., C. D. Canham, M. Beaudet, and C. Messier. 2010. Shade tolerance, canopy gaps and mechanisms of coexistence of forest trees. Oikos 119:475–484.

Hanbury-Brown, A. R., R. E. Ward, and L. M. Kueppers. 2022. Forest regeneration within Earth system models: current process representations and ways forward. New Phytologist 235:20–40.

Harrison, S. P., W. Cramer, O. Franklin, I. C. Prentice, H. Wang, A. Brannstrom, H. de Boer, U. Dieckmann, J. Joshi, T. F. Keenan, A. Lavergne, S. Manzoni, G. Mengoli, C. Morfopoulos, J. Penuelas, S. Pietsch, K. T. Rebel, Y. Ryu, N. G. Smith, B. D. Stocker, and I. J. Wright. 2021. Eco-evolutionary optimality as a means to improve vegetation and land-surface models. New Phytologist 231:2125–2141.

Hodgkins, E. J., and N. G. Nichols. 1977. Extent of main lateral roots in natural longleaf pine as related to position and age of trees. Forest Science 23:161–166.

Hubau, W., S. L. Lewis, O. L. Phillips, K. Affum-Baffoe, H. Beeckman, A. Cuni-Sanchez, A. K. Daniels, C. E. N. Ewango, S. Fauset, J. M. Mukinzi, D. Sheil, B. Sonke, M. J. P. Sullivan, T. C. H. Sunderland, H. Taedoumg, S. C. Thomas, L. J. T. White, K. A. Abernethy, S. Adu-Bredu, C. A. Amani, T. R. Baker, L. F. Banin, F. Baya, S. K. Begne, A. C. Bennett, F. Benedet, R. Bitariho, Y. E. Bocko, P. Boeckx, P. Boundja, R. J. W. Brienen, T. Brncic, E. Chezeaux, G. B. Chuyong, C. J. Clark, M. Collins, J. A. Comiskey, D. A. Coomes, G. C. Dargie, T. de Haulleville, M. N. D. Kamdem, J.-L. Doucet, A. Esquivel-Muelbert, T. R. Feldpausch, A. Fofanah, E. G. Foli, M. Gilpin, E. Gloor, C. Gonmadje, S. Gourlet-Fleury, J. S. Hall, A. C. Hamilton, D. J. Harris, T. B. Hart, M. B. N. Hockemba, A. Hladik, S. A. Ifo, K. J. Jeffery, T. Jucker, E. K. Yakusu, E. Kearsley, D. Kenfack, A. Koch, M. E. Leal, A. Levesley, J. A. Lindsell, J. Lisingo, G. Lopez-Gonzalez, J. C. Lovett, J.-R. Makana, Y. Malhi, A. R. Marshall, J. Martin, E. H. Martin, F. M. Mbayu, V. P. Medjibe, V. Mihindou, E. T. A. Mitchard, S. Moore, P. K. T. Munishi, N. N. Bengone, L. Ojo, F. E. Ondo, K. S.-H. Peh, G. C. Pickavance, A. D. Poulsen, J. R. Poulsen, L. Qie, J. Reitsma, F. Rovero, M. D. Swaine, J. Talbot, J. Taplin, D. M. Taylor, D. W. Thomas, B. Toirambe, J. T. Mukendi, D. Tuagben, P. M. Umunay, G. M. F. van der Heijden, H. Verbeeck, J. Vleminckx, S. Willcock, H. Woll, J. T. Woods, and L. Zemagho. 2020. Asynchronous carbon sink saturation in African and Amazonian tropical forests. Nature 579:80–87.

King, D. A. 1993. A model analysis of the influence of root and foliage allocation on forest production and competition between trees. Tree Physiology 12:119–135.

Koven, C. D., R. G. Knox, R. A. Fisher, J. Q. Chambers, B. O. Christoffersen, S. J. Davies, M. Detto, M. C. Dietze, B. Faybishenko, J. Holm, M. Huang, M. Kovenock, L. M. Kueppers, G. Lemieux, E. Massoud, N. G. McDowel, H. C. Muller-Landau, J. F. Needham, R. J. Norby, T. Powell, A. Rogers, S. P. Serbin, J. K. Shuman, A. L. S. Swann, C. Varadharajan, A. P. Walker, S. J. Wright, and C. Xu. 2020. Benchmarking and parameter sensitivity of physiological and vegetation dynamics using the Functionally Assembled Terrestrial Ecosystem Simulator (FATES) at Barro Colorado Island, Panama. Biogeosciences 17:3017–3044.

Kozlowski, T. T., and S. G. Pallardy. 2002. Acclimation and adaptive responses of woody plants to environmental stresses. Botanical Review 68:270–334.

Langan, L., S. I. Higgins, and S. Scheiter. 2017. Climate-biomes, pedo-biomes or pyro-biomes: which world view explains the tropical forest-savanna boundary in South America? Journal of Biogeography 44:2319–2330.

Leuning, R. 1995. A critical appraisal of a combined stomatal-photosynthesis model for C_3 plants. Plant, Cell and Environment 18:339–355.

Levine, N. M., K. Zhang, M. Longo, A. Baccini, O. L. Phillips, S. L. Lewis, E. Alvarez-Davila, A. C. Segalin de Andrade, R. J. W. Brienen, T. L. Erwin, T. R. Feldpausch, A. L. Monteagudo Mendoza, P. Nunez Vargas, A. Prieton, J. Eduardo Silva-Espejo, Y. Malhi, and P. R. Moorcroft. 2016. Ecosystem heterogeneity determines the ecological resilience of the Amazon to climate change. Proceedings of the National Academy of Sciences 113:793–797.

Lichstein, J. W., N.-Z. Golaz, S. Malyshev, E. Shevliakova, T. Zhang, J. Sheffield, R. A. Birdsey, J. L. Sarmiento, and S. W. Pacala. 2014. Confronting terrestrial biosphere models with forest inventory data. Ecological Applications 24:699–715.

Lichstein, J. W., and S. W. Pacala. 2011. Local diversity in heterogeneous landscapes: quantitative assessment with a height-structured forest metacommunity model. Theoretical Ecology 4:269–281.

Lichstein, J. W., T. Zhang, E. Weng, C. E. Farrior, R. Dybzinski, S. Malyshev, E. Shevliakova, R. A. Birdsey, and S. W. Pacala. 2024. Data and code archive for: Effects of water limitation and competition on tree carbon allocation in an Earth system modeling framework. In Journal of Ecology. Zenodo. https://doi.org/10.5281/zenodo.13376013.

Malhi, Y., C. Doughty, and D. Galbraith. 2011. The allocation of ecosystem net primary productivity in tropical forests. Philosophical Transactions of the Royal Society B-Biological Sciences 366:3225–3245.

Martínez Cano, I., E. Shevliakova, S. Malyshev, S. J. Wright, M. Detto, S. W. Pacala, and H. C. Muller-Landau. 2020. Allometric constraints and competition enable the simulation of size structure and carbon fluxes in a dynamic vegetation model of tropical forests (LM3PPA-TV). Global Change Biology 26:4478–4494.

McDowell, N. G., R. A. Fisher, C. Xu, J. C. Domec, T. Holtta, D. S. Mackay, J. S. Sperry, A. Boutz, L. Dickman, N. Gehres, J. M. Limousin, A. Macalady, J. Martinez-Vilalta, M. Mencuccini, J. A. Plaut, J. Ogee, R. E. Pangle, D. P. Rasse, M. G. Ryan, S. Sevanto, R. H. Waring, A. P. Williams, E. A. Yepez, and W. T. Pockman. 2013. Evaluating theories of drought-induced vegetation mortality using a multimodel-experiment framework. New Phytologist 200:304–321.

Meador, W. E., and W. R. Weaver. 1980. Two-stream approximations to radiative transfer in planetary atmospheres: a unified description of existing methods and a new improvement. Journal of the Atmospheric Sciences 37:630–643.

Moorcroft, P. R. 2006. How close are we to a predictive science of the biosphere? Trends in Ecology & Evolution 21:400–407.

Moorcroft, P. R., G. C. Hurtt, and S. W. Pacala. 2001. A method for scaling vegetation dynamics: The ecosystem demography model (ED). Ecological Monographs 71:557–585.

Ostle, N., P. Smith, R. Fisher, F. Woodward, J. Fisher, J. Smith, D. Galbraith, P. Levy, P. Meir, N. McNamara, and R. Bardgett. 2009. Integrating plant-soil interactions into global carbon cycle models. Journal of Ecology 97:851–863.

Pacala, S. W., C. D. Canham, J. Saponara, J. A. Silander, R. K. Kobe, and E. Ribbens. 1996. Forest models defined by field measurements: estimation, error analysis and dynamics. Ecological Monographs 66:1–43.

Pan, Y., R. A. Birdsey, J. Fang, R. Houghton, P. E. Kauppi, W. A. Kurz, O. L. Phillips, A. Shvidenko, S. L. Lewis, J. G. Canadell, P. Ciais, R. B. Jackson, S. W. Pacala, A. D. McGuire, S. Piao, A. Rautiainen, S. Sitch, and D. Hayes. 2011a. A large and persistent carbon sink in the world's forests. Science 333:988–993.

Pan, Y., J. M. Chen, R. Birdsey, K. McCullough, L. He, and F. Deng. 2011b. Age structure and disturbance legacy of North American forests. Biogeosciences 8:715–732.

Poorter, H., K. J. Niklas, P. B. Reich, J. Oleksyn, P. Poot, and L. Mommer. 2012. Biomass allocation to leaves, stems and roots: meta-analyses of interspecific variation and environmental control. New Phytologist 193:30–50.

Raupach, M. R., P. J. Rayner, D. J. Barrett, R. S. DeFries, M. Heimann, D. S. Ojima, S. Quegan, and C. C. Schmullius. 2005. Model-data synthesis in terrestrial carbon observation: methods, data requirements and data uncertainty specifications. Global Change Biology 11:378–397.

Reichstein, M., M. Bahn, P. Ciais, D. Frank, M. D. Mahecha, S. I. Seneviratne, J. Zscheischler, C. Beer, N. Buchmann, D. C. Frank, D. Papale, A. Rammig, P. Smith, K. Thonicke, M. van der Velde, S. Vicca, A. Walz, and M. Wattenbach. 2013. Climate extremes and the carbon cycle. Nature 500:287–295.

Running, S. W., and M. Zhao. 2015. Daily GPP and annual NPP (MOD17A2/A3) products NASA Earth Observing System MODIS land algorithm. MOD17 User's Guide 2015:1–28.

Sakschewski, B., W. von Bloh, A. Boit, L. Poorter, M. Pena-Claros, J. Heinke, J. Joshi, and K. Thonicke. 2016. Resilience of Amazon forests emerges from plant trait diversity. Nature Climate Change 6:1032–1036.

Sakschewski, B., W. von Bloh, A. Boit, A. Rammig, J. Kattge, L. Poorter, J. Penuelas, and K. Thonicke. 2015. Leaf and stem economics spectra drive diversity of functional plant traits in a dynamic global vegetation model. Global Change Biology 21:2711–2725.

Scheiter, S., L. Langan, and S. I. Higgins. 2013. Next-generation dynamic global vegetation models: learning from community ecology. New Phytologist 198:957–969.

Sheffield, J., G. Goteti, and E. F. Wood. 2006. Development of a 50-year high-resolution global dataset of meteorological forcings for land surface modeling. Journal of Climate 19:3088–3111.

Shinozaki, K., K. Yoda, K. Hozumi, and T. Kira. 1964. A quantitative analysis of plant form - The pipe model theory I. Basic Analyses. Japanese Journal of Ecology 14:97–105.

Sitch, S., C. Huntingford, N. Gedney, P. E. Levy, M. Lomas, S. L. Piao, R. Betts, P. Ciais, P. Cox, P. Friedlingstein, C. D. Jones, I. C. Prentice, and F. I. Woodward. 2008. Evaluation of the terrestrial carbon cycle, future plant geography and climate-carbon cycle feedbacks using five Dynamic Global Vegetation Models (DGVMs). Global Change Biology 14:2015–2039.

Smith, B., I. C. Prentice, and M. T. Sykes. 2001. Representation of vegetation dynamics in the modelling of terrestrial ecosystems: comparing two contrasting approaches within European climate space. Global Ecology and Biogeography 10:621–637.

Strigul, N., D. Pristinski, D. Purves, J. Dushoff, and S. Pacala. 2008. Scaling from trees to forests: tractable macroscopic equations for forest dynamics. Ecological Monographs 78:523–545.

Vitousek, P. M., and R. W. Howarth. 1991. Nitrogen limitation on land and in the sea: How can it occur? Biogeochemistry 13:87–115.

Vitousek, P. M., S. Porder, B. Z. Houlton, and O. A. Chadwick. 2010. Terrestrial phosphorus limitation: mechanisms, implications, and nitrogen-phosphorus interactions. Ecological Applications 20:5–15.

Wang, H., I. C. Prentice, T. F. Keenan, T. W. Davis, I. J. Wright, W. K. Cornwell, B. J. Evans, and C. Peng. 2017. Towards a universal model for carbon dioxide uptake by plants. Nature Plants 3:734–741.

Weng, E., and Y. Luo. 2008. Soil hydrological properties regulate grassland ecosystem responses to multifactor global change: A modeling analysis. Journal of Geophysical Research-Biogeosciences 113:G03003.

Weng, E. S., R. Dybzinski, C. E. Farrior, and S. W. Pacala. 2019. Competition alters predicted forest carbon cycle responses to nitrogen availability and elevated CO_2: simulations using an explicitly competitive, game-theoretic vegetation demographic model. Biogeosciences 16:4577–4599.

Weng, E. S., C. E. Farrior, R. Dybzinski, and S. W. Pacala. 2017. Predicting vegetation type through physiological and environmental interactions with leaf traits: evergreen and deciduous forests in an earth system modeling framework. Global Change Biology 23:2482–2498.

Weng, E. S., S. Malyshev, J. W. Lichstein, C. E. Farrior, R. Dybzinski, T. Zhang, E. Shevliakova, and S. W. Pacala. 2015. Scaling from individual trees to forests in an Earth system modeling framework using a mathematically tractable model of height-structured competition. Biogeosciences 12:2655–2694.

Wolf, A., W. R. L. Anderegg, and S. W. Pacala. 2016. Optimal stomatal behavior with competition for water and risk of hydraulic impairment. Proceedings of the National Academy of Sciences 113:E7222–E7230.

Wullschleger, S. D., H. E. Epstein, E. O. Box, E. S. Euskirchen, S. Goswami, C. M. Iversen, J. Kattge, R. J. Norby, P. M. van Bodegom, and X. Xu. 2014. Plant functional types in Earth system models: past experiences and future directions for application of dynamic vegetation models in high-latitude ecosystems. Annals of Botany 114:1–16.

Zaehle, S., and A. D. Friend. 2010. Carbon and nitrogen cycle dynamics in the O-CN land surface model: 1. Model description, site-scale evaluation, and sensitivity to parameter estimates. Global Biogeochemical Cycles 24:GB1005.

Zhang, L., W. R. Dawes, and G. R. Walker. 2001. Response of mean annual evapotranspiration to vegetation changes at catchment scale. Water Resources Research 37:701–708.

Zhang, T., Ü. Niinemets, J. Sheffield, and J. W. Lichstein. 2018. Shifts in tree functional composition amplify the response of forest biomass to climate. Nature 556:99–102.

Zorzetto, E., S. Malyshev, N. Chaney, D. Paynter, R. Menzel, and E. Shevliakova. 2023. Effects of complex terrain on the shortwave radiative balance: a sub-grid-scale parameterization for the GFDL Earth System Model version 4.1. Geoscientific Model Development 16:1937–1960.

Table 1. Key terms and abbreviations.

Abbreviation	Description
φ_{RL}	Ratio of fine-root surface area to leaf area for a tree cohort. This ratio and LAI_{max} together define an allocation strategy ('variant') for a given set of vegetation parameters (*Acer* or *Populus*; Table S1).
LAI_{max}	Target leaf area index (leaf area per crown area) for a tree cohort. LAI_{max} and the root:leaf ratio (φ_{RL}) together define an allocation strategy ('variant') for a given set of vegetation parameters (*Acer* or *Populus*; Table S1).
competitive strategy	The competitively dominant set of traits, equivalent to an evolutionarily stable strategy (ESS) and represented in our study by S_{COMP}[†].
maximizing strategy	A set of traits that maximizes some aspect of ecosystem functioning or performance in monoculture (i.e., in the absence of interspecific competition), represented in our study by S_{AGB}, S_{NPP}, S_{NPPw}, and S_{DT}.
optimal strategy	A set of traits that is optimal in some sense. An optimal strategy may be a competitive strategy, a maximizing strategy, or both (in cases where they converge).
S_{COMP}	Most competitive strategy at equilibrium[‡]. This allocation strategy outcompetes all others under a given climate and in the absence of exogenous disturbance; i.e., the only sources of mortality are background mortality, carbon starvation, and the direct effects of water deficit (Eq. 1).

S_{AGB}	Biomass-maximizing strategy at equilibrium. This allocation strategy maximizes aboveground wood biomass (AGB) in monoculture at equilibrium. In the LM3-PPA and BiomeE models, coarse root biomass is assumed proportional to AGB, so S_{AGB} also maximizes total wood biomass.
S_{NPP}	Productivity-maximizing strategy at equilibrium. This allocation strategy maximizes total net primary production (above plus belowground) in monoculture at equilibrium.
S_{NPPw}	Wood-productivity-maximizing strategy at equilibrium. This allocation strategy maximizes the rate of wood production (i.e., NPP that is allocated to wood) in monoculture at equilibrium. S_{NPPw} was identified in BiomeE experiments only.
S_{DT}	Most drought-tolerant strategy. This allocation strategy maximizes AGB in monocultures exposed to novel drought.

† We conjecture that each S_{COMP} identified in our LM3-PPA and BiomeE experiments corresponds to an ESS, but formally demonstrating this would require additional experiments to show that (*i*) S_{COMP} (as a resident at equilibrium) resists invasion by all other strategies and (*ii*) S_{COMP} can invade a resident population of any other strategy.

‡ Equilibrium conditions were estimated by averaging over the last 100 years of long-term simulations (quasi-equilibrium period). For LM3-PPA, long-term experiments lasted 500 years for monoculture and pairwise competition experiments. For BiomeE, long-term experiments lasted 500 years for monocultures and 1244 years for 30-strategy polycultures.

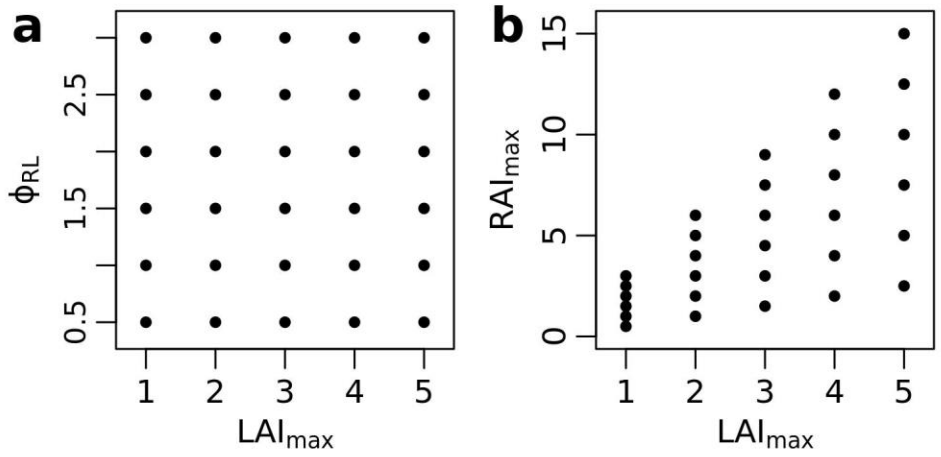

Figure 1. (a) The 30 allocational strategies ('variants') for canopy trees considered in LM3-PPA and BiomeE experiments were defined by combinations of two allocational traits: target leaf area index of an individual's crown (LAI_{max}) and root:leaf ratio (φ_{RL}; ratio of fine-root surface area to leaf area). (b) The same trait space, with the *y*-axis expressed as fine-root surface area per-unit crown area ($RAI_{max} = LAI_{max} \times \varphi_{RL}$). All understory trees were assumed to share the same allocational strategy ($LAI_{max} = 1$; $\varphi_{RL} = 0.5$).

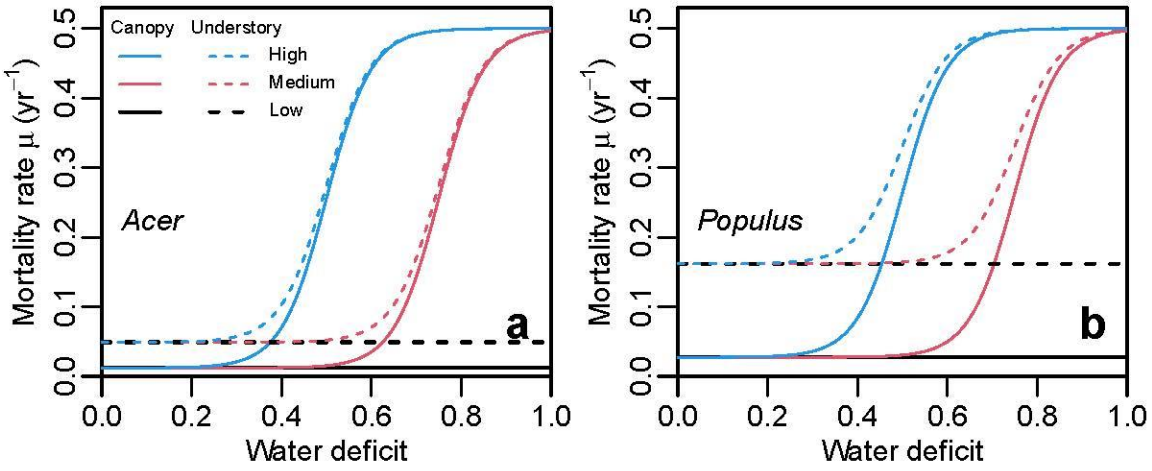

Figure 2. Three alternative model scenarios for (a) *Acer* and (b) *Populus* for the sensitivity of annual tree mortality rate to water deficit (Eq. 1): low (black), medium (red), and high sensitivity (blue). The *x*-axis (relative water deficit, *d* in Eq. 1) is the ratio, for a given year, between cumulative water deficit (demand minus supply) and cumulative water demand, which depends on the traits of the individuals in a cohort, competition with other cohorts, and abiotic conditions. The horizontal lines (low sensitivity of mortality to water deficit) show baseline mortality rates (Table S1). In the medium and high sensitivity scenarios, mortality approaches an assumed asymptote of 0.5 yr^{-1} with increasing water deficit. Mortality due to carbon starvation is an additional mortality mechanism not included in this figure and can, in principle, occur in all model scenarios due to water and/or light limitation.

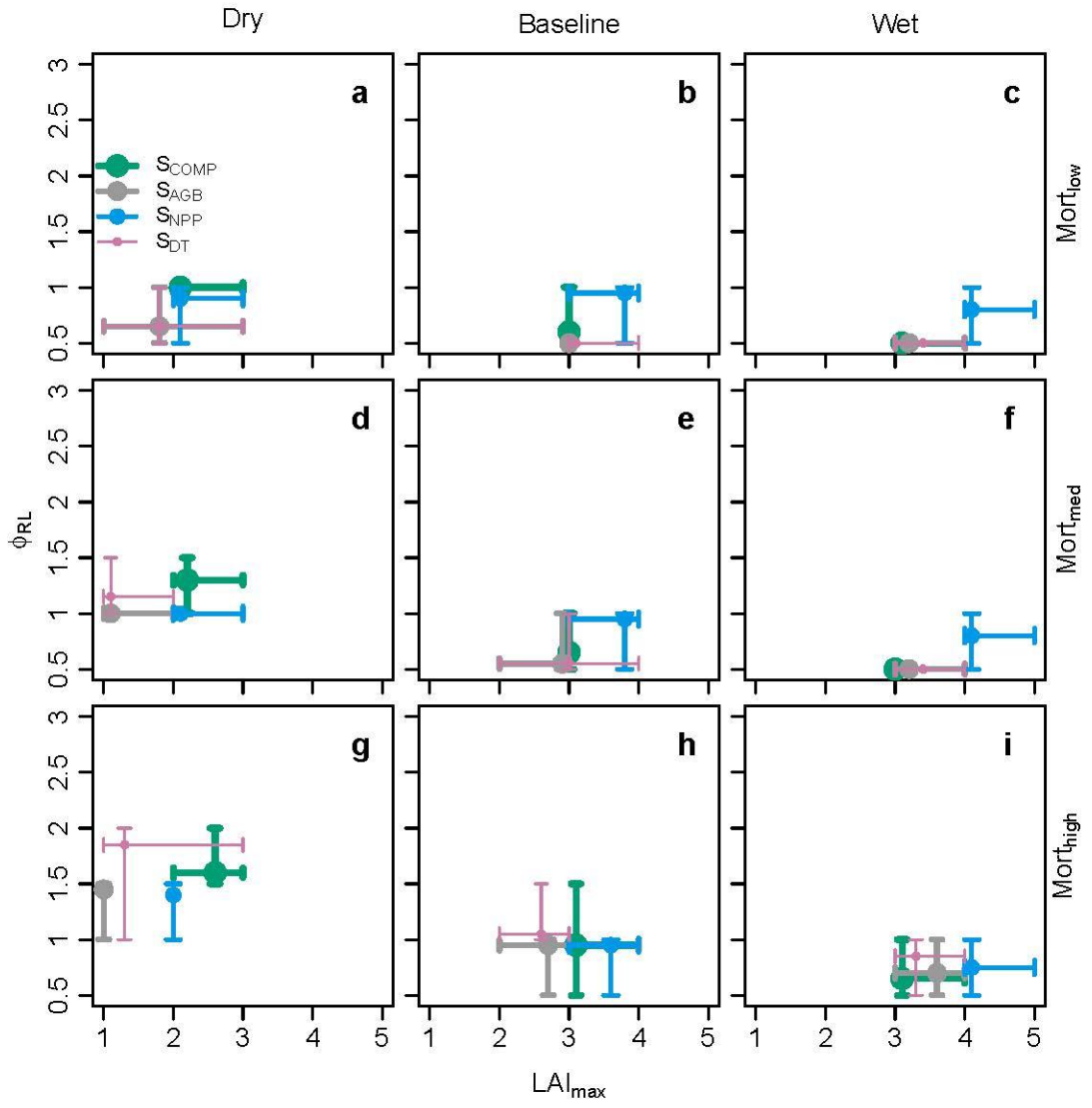

Figure 3. LM3-PPA model predictions, with *Acer* parameter values, for the most competitive (S_{COMP}), biomass-maximizing (S_{AGB}), NPP-maximizing (S_{NPP}), and most drought-tolerant (S_{DT}) strategies in the trait space defined by the target leaf area index of a crown (LAI_{max}) and the root:leaf area ratio (φ_{RL}). Columns represent dry (0.5×), baseline (1×), and wet (1.5×) precipitation scenarios. Rows represent low, medium, and high sensitivity of mortality to water deficit (Fig. 2). Points and error bars show trait means and ranges across sites (Fig. S1). The large ranges reflect deterministic effects of site differences in climate (the model is deterministic,

and soils were assumed uniform across sites). Corresponding LM3-PPA results for *Populus* are in Fig. S5, and corresponding BiomeE results are in Figs. S6-S9.

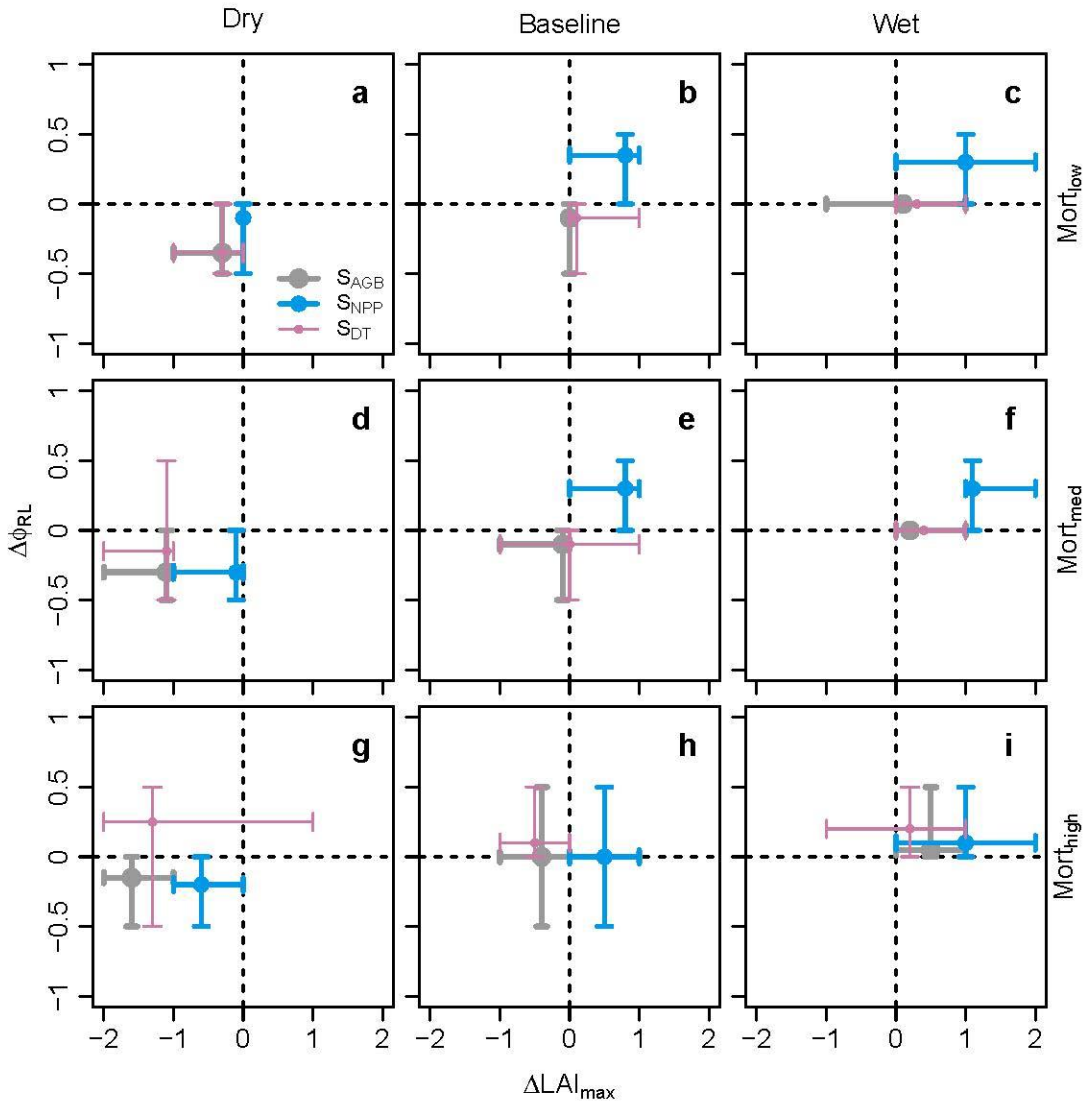

Figure 4. LM3-PPA model predictions, with *Acer* parameter values, for differences in trait values between maximizing strategies (S_{AGB}, S_{NPP}, and S_{DT}) and the most competitive strategy (S_{COMP}). Axes are differences in trait values shown in Fig. 3 (maximizing value minus S_{COMP} value). Points and error bars show means and ranges of differences across sites (Fig. S1). Other details as in Fig. 3. Corresponding LM3-PPA results for *Populus* are in Fig. S10, and corresponding BiomeE results are in Figs. S11-S14.

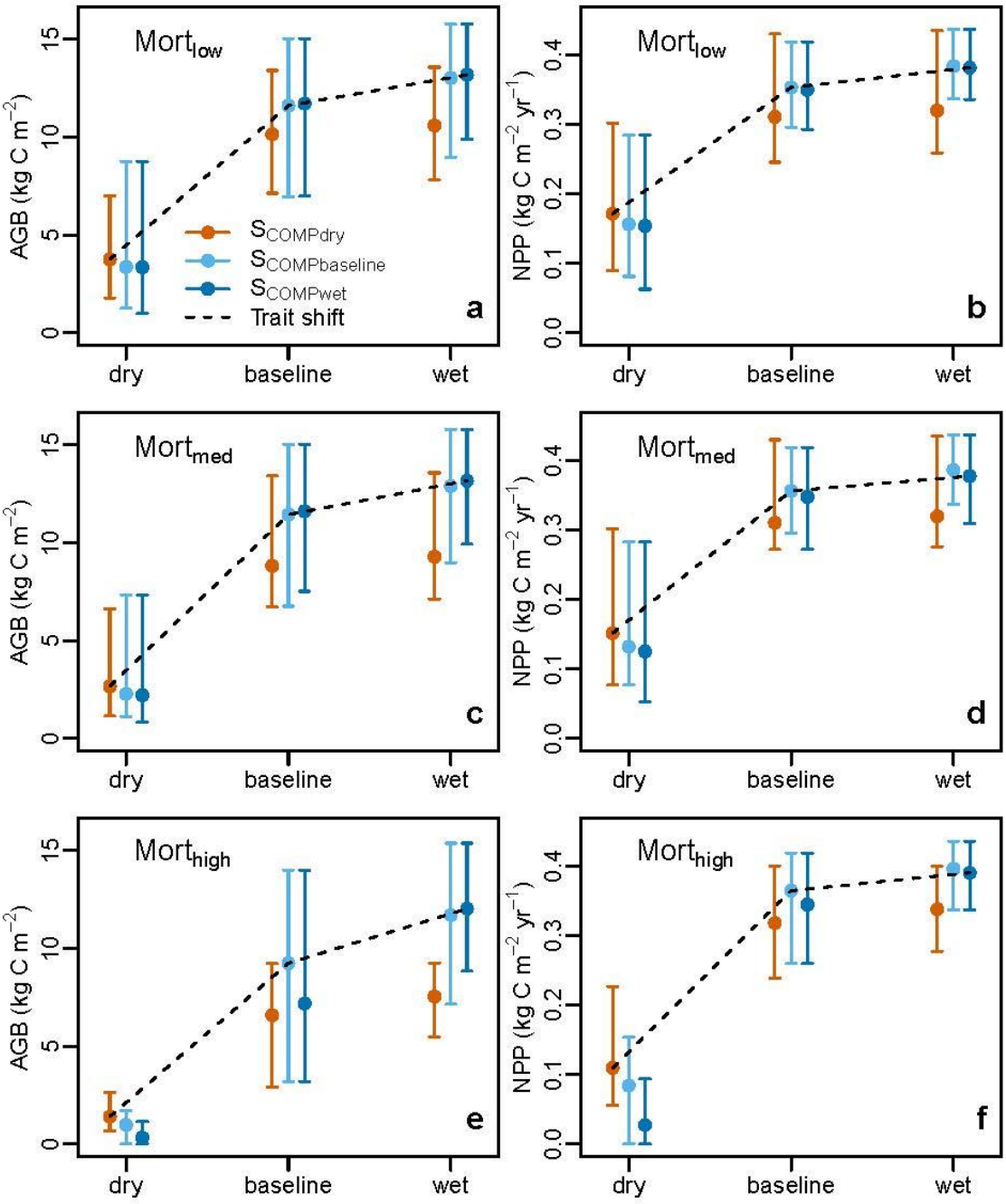

Figure 5. LM3-PPA model predictions, with *Acer* parameter values, for effects of trait shifts on stand-level aboveground wood biomass (AGB; left) and net primary productivity (NPP; right). $S_{COMPdry}$, $S_{COMPbaseline}$, and $S_{COMPwet}$ are the most competitive strategies under the dry (0.5×), baseline (1×), and wet (1.5×) precipitation scenarios, respectively. The dashed line shows the mean ecosystem response to climate assuming climate-driven shifts in S_{COMP}. Rows represent

low, medium, and high sensitivity of mortality to water deficit (Fig. 2). Points and error bars show means and ranges of stand-level AGB and NPP across sites (Fig. S1). Cases where error bars extend to zero indicate one or more inviable strategies (in the high-mortality scenario, $S_{COMPbaseline}$ was not viable under dry climate at 1/10 sites, and $S_{COMPwet}$ was not viable under dry climate at 6/10 sites). Corresponding LM3-PPA results for *Populus* are in Fig. S15, and corresponding BiomeE results are in Figs. S16-S19.

Graphical abstract:

1) The theoretical prediction that competitive and maximizing allocation strategies differ under water limitation is confirmed for a demographic model designed as an ESM component. Optimality-based trait predictions can simplify representing trait diversity in ESMs but do not always correspond to competitive outcomes. Explicitly modeling coexistence and community assembly in ESMs is challenging but is likely the most general approach to representing trait diversity.